Pulmonary surfactant proteins are inhibited by IgA autoantibodies in severe COVID-19

Tobias Sinnberg[1,2,3,*], Christa Lichtensteiger[4,*], Omar Hasan Ali[4,5,6,*], Oltin T. Pop[4], Ann-Kristin Jochum[4,7], Lorenz Risch[8,9,10], Silvio D. Brugger[11], Ana Velic[12], David Bomze[4,13], Philipp Kohler[14], Pietro Vernazza[14], Werner C. Albrich[14], Christian R. Kahlert[14,15], Marie-Therese Abdou[4], Nina Wyss[4], Kathrin Hofmeister[1], Heike Niessner[1,2], Carl Zinner[16], Mara Gilardi[16], Alexandar Tzankov[16], Martin Röcken[1,2], Alex Dulovic[17], Srikanth Mairpady Shambat[11], Natalia Ruetalo[18], Philipp K. Buehler[19], Thomas C. Scheier[11], Wolfram Jochum[7], Lukas Kern[20], Samuel Henz[21], Tino Schneider[22], Gabriela M. Kuster[23], Maurin Lampart[23], Martin Siegemund[24,25], Roland Bingisser[26], Michael Schindler[18], Nicole Schneiderhan-Marra[17], Hubert Kalbacher[27], Kathy D. McCoy[28], Werner Spengler[29], Martin H. Brutsche[19], Boris Maček[12], Raphael Twerenbold[22,30], Josef M. Penninger[5,31], Matthias S. Matter[8], and Lukas Flatz[1,4,6,32]

Affiliations

[1]Department of Dermatology, University Hospital Tübingen, Tübingen, 72076, Germany.

[2]Cluster of Excellence iFIT (EXC 2180) Image Guided and Functionally Instructed Tumor Therapies, University Hospital Tübingen, Tübingen, 72074, Germany.

[3]Department of Dermatology, Venereology and Allergology, Charité-Universitätsmedizin Berlin, Charitéplatz 1, 10117 Berlin, Germany.

[4]Institute of Immunobiology, Cantonal Hospital St. Gallen, St. Gallen, 9007, Switzerland.

[5]Department of Medical Genetics, Life Sciences Institute, University of British Columbia, Vancouver, British Columbia, V6T 1Z3, Canada.

AJRCCM Articles in Press. Published August 04, 2022 as 10.1164/rccm.202201-0011OC

[6]Department of Dermatology, University Hospital Zurich, University of Zurich, Zurich, 8091, Switzerland.

[7]Institute of Pathology, Cantonal Hospital St. Gallen, St. Gallen, 9007, Switzerland.

[8]Center of Laboratory Medicine Dr Risch, Vaduz, 9490, Liechtenstein.

[9]Center of Laboratory Medicine, University Institute of Clinical Chemistry, University Hospital Bern, University of Bern, Bern, 3010, Switzerland.

[10]Faculty of Medical Sciences, Private University in the Principality of Liechtenstein, 9495, Liechtenstein.

[11]Department of Infectious Diseases and Hospital Hygiene, University Hospital Zurich, University of Zurich, Zurich, 8091, Switzerland.

[12]Proteome Center Tübingen, Interfaculty Institute for Cell Biology, University of Tübingen, Tübingen, 72076, Germany.

[13]Sackler Faculty of Medicine, Tel Aviv University, Tel Aviv, 6997801, Israel.

[14]Division of Infectious Diseases and Hospital Epidemiology, Cantonal Hospital St. Gallen, St. Gallen, 9007, Switzerland.

[15]Department of Infectious Diseases and Hospital Epidemiology, Children's Hospital of Eastern Switzerland, St. Gallen, 9000, Switzerland.

[16]Pathology, Institute of Medical Genetics and Pathology, University Hospital Basel, University of Basel, Basel, 4031, Switzerland.

[17]NMI Natural and Medical Sciences Institute at the University of Tübingen, Reutlingen, 72770, Germany.

[18]Institute for Medical Virology and Epidemiology, University Hospital Tübingen, Tübingen, 72076, Germany.

AJRCCM Articles in Press. Published August 04, 2022 as 10.1164/rccm.202201-0011OC

[19]Institute of Intensive Care Medicine, University Hospital Zurich, University of Zurich, Zurich, 8091, Switzerland.

[20]Lung Center, Cantonal Hospital St. Gallen, St. Gallen, 9007, Switzerland.

[21]Department of Internal Medicine, Cantonal Hospital St. Gallen, St. Gallen, 9007, Switzerland.

[22]Division of Pneumology, Cantonal Hospital St. Gallen, St. Gallen, 9007, Switzerland.

[23]Department of Cardiology and Cardiovascular Research Institute Basel (CRIB), University Hospital Basel, University of Basel, Basel, 4056, Switzerland.

[24]Intensive Care Unit, Department of Acute Medicine, University Hospital Basel, University of Basel, Basel, 4031, Switzerland.

[25]Department of Clinical Research, University Hospital Basel, University of Basel, Basel, 4031, Switzerland.

[26]Emergency Department, University Hospital Basel, University of Basel, Basel, 4031, Switzerland.

[27]Institute of Clinical Anatomy and Cell Analysis, University of Tübingen, Tübingen, 72074, Germany.

[28]Snyder Institute for Chronic Disease, Cumming School of Medicine, University of Calgary, Calgary, Alberta, T2N 4N1, Canada.

[29]Department of Medical Oncology and Pneumology, University Hospital Tübingen, Tübingen, 72076, Germany.

[30]University Center of Cardiovascular Science and Department of Cardiology, University Heart and Vascular Center Hamburg, University Medical Center Hamburg-Eppendorf, Partner Site Hamburg-Kiel-Lübeck, Hamburg, 20251, Germany.

AJRCCM Articles in Press. Published August 04, 2022 as 10.1164/rccm.202201-0011OC

[31]Institute of Molecular Biotechnology of the Austrian Academy of Sciences (IMBA), Vienna, 1030, Austria.

[32]Department of Dermatology, Venereology and Allergology, Cantonal Hospital St. Gallen, St. Gallen, 9007, Switzerland.

[*]These authors contributed equally.

Corresponding author:

Prof. Lukas Flatz, M.D.

University Hospital Tübingen, Department of Dermatology

Liebermeisterstraße 25, 72076 Tübingen, Germany

Phone: +49 152 51869358 Email: lukas.flatz@med.uni-tuebingen.de

Author contributions

These authors contributed equally: T.S., C.L., and O.H.A.

Conceptualization and study planning: L.F., T.S., C.L. O.H.A., and M.S.M.

Methodology: T.S., L.F., O.T.P., M.G., L.R., D.B., C.Z., H.K., A.T., A.V., B.M., C.D.M., M.S., M.R., and J.M.P.

Sample collection and experimentation: T.S., C.L., O.H.A., O.T.P., A.-K.J., R.T., M.L., M.G., P.K., P.V., W.C.A., C.R.K., S.D.B., M.-T.A., K.H., A.D., S.M.-S., P.K.B., T.C.S., W.J., L.K., S.H., G.M.K., M.S., R.B., M.H.B., N.S-M., K.M, A.V., N.R., T.Sch., W.S. and B.M.

Statistical analysis: T.S, O.H.A. and D.B.

Data visualization: T.S., O.H.A., O.T.P., C.Z., D.B., and M.G.

Initial version of the manuscript: O.H.A, T.S., and C.L.

Final manuscript: All authors.

AJRCCM Articles in Press. Published August 04, 2022 as 10.1164/rccm.202201-0011OC

Sources of support

LF is supported by grants from the Swiss National Science Foundation (PP00P3_157448), the Research Fund of the Cantonal Hospital St. Gallen (20/20), and the Lungenliga St. Gallen–Appenzell. TS received support by Germany's excellence strategy, EXC 2180-390900677, Image Guided and Functionally Instructed Tumor Therapies (iFIT). OHA is supported by a Swiss National Science Foundation grant (P400PM_194473). MSM is supported by a grant from the Swiss National Science Foundation (320030_189275) and a Botnar Foundation Research Centre for Child Health Emergency Response to COVID-19 grant. PK is supported by a Swiss National Science Foundation grant (PZ00P3_179919). SDB is supported by a Promedica Foundation grant (1449/M). CZ and AT received a Botnar Foundation Research Centre for Child Health Emergency Response to COVID-19 grant. RT has received a Swiss National Science Foundation grant (P300PB_167803) and is supported by the Swiss Heart Foundation, the Cardiovascular Research Foundation Basel, and an unrestricted research grant from Roche Diagnostics. JMP has received a T. von Zastrow Foundation grant, an Austrian Science Fund - FWF Wittgenstein award (Z 271-B19), the Innovative Medicines Initiative 2 Joint Undertaking (JU) program grant (101005026), the Canada 150 Research Chairs Program grant (F18-01336), and Canadian Institutes of Health Research COVID-19 grants (F20-02343, F20-02015), and is supported by the Austrian Academy of Sciences.

Running title: Autoantibodies against surfactant proteins in COVID-19

AJRCCM Articles in Press. Published August 04, 2022 as 10.1164/rccm.202201-0011OC

Subject category: 10.14 Pneumonia viral infections

Total word count (excluding abstract, references, figure legends): 3171

At a Glance Commentary

Scientific Knowledge on the Subject: Severe coronavirus disease (COVID-19) can lead to fatal acute respiratory distress syndrome. While it has been shown that COVID-19 can induce autoimmunity, there are limited data on autoantibodies in the lungs and their contribution to COVID-19 severity.

What This Study Adds to the Field: This multicenter cross-sectional study shows that COVID-19 patients with severe disease harbor IgA autoantibodies targeting pulmonary surfactant proteins B and C. Furthermore, the presence of these IgA in pulmonary surfactant interferes with its capability to reduce surface tension. These results suggest that IgA autoantibodies directed against surfactant proteins contribute to COVID-19 severity.

This article has an online data supplement, which is accessible from this issue's table of content online at www.atsjournals.org.

AJRCCM Articles in Press. Published August 04, 2022 as 10.1164/rccm.202201-0011OC

Some of the results of these studies have been previously reported in the form of a preprint (bioRxiv, 7 February 2021 https://doi.org/10.1101/2021.02.02.21250940)

AJRCCM Articles in Press. Published August 04, 2022 as 10.1164/rccm.202201-0011OC

Abstract

Rationale:

Coronavirus disease 2019 (COVID-19) can lead to acute respiratory distress syndrome with fatal outcomes. Evidence suggests that dysregulated immune responses, including autoimmunity, are key pathogenic factors.

Objectives:

To assess whether IgA autoantibodies target lung-specific proteins and contribute to disease severity.

Methods:

We collected 147 blood, 9 lung tissue, and 36 bronchoalveolar lavage fluid samples from three tertiary hospitals in Switzerland and one in Germany. Severe COVID-19 was defined by the need to administer oxygen. We investigated the presence of IgA autoantibodies and their effects on pulmonary surfactant in COVID-19 using the following methods: immunofluorescence on tissue samples, immunoprecipitations followed by mass spectrometry on bronchoalveolar lavage fluid samples, enzyme-linked immunosorbent assays on blood samples, and surface tension measurements with medical surfactant.

Measurements and Main Results:

IgA autoantibodies targeting pulmonary surfactant proteins B and C were elevated in patients with severe COVID-19, but not in patients with influenza or bacterial pneumonia. Notably, pulmonary surfactant failed to reduce surface tension after incubation with either plasma or purified IgA from patients with severe COVID-19.

Conclusions:

AJRCCM Articles in Press. Published August 04, 2022 as 10.1164/rccm.202201-0011OC

Our data suggest that patients with severe COVID-19 harbor IgA against pulmonary surfactant proteins B and C and that these antibodies block the function of lung surfactant, potentially contributing to alveolar collapse and poor oxygenation.

Abstract word count: 207

Keywords

COVID-19; SARS-CoV-2; autoimmunity; immunoglobulin A; pulmonary surfactant; pulmonary-associated surfactant protein

AJRCCM Articles in Press. Published August 04, 2022 as 10.1164/rccm.202201-0011OC

Introduction

Coronavirus disease 2019 (COVID-19) is caused by infection with severe acute respiratory syndrome coronavirus 2 (SARS-CoV-2) and has rapidly evolved into a global pandemic (1, 2). While the introduction of effective vaccines against SARS-CoV-2 has had a major impact on fighting the disease (3-6) it remains a burden on health care systems as a high vaccination coverage has yet to be achieved in most countries (7). Dysfunctional immune responses and early alveolar damage are thought to play a determining role in COVID-19 progression (8, 9). In the lungs, severe COVID-19 is characterized by the following features: cell pyroptosis that occurs due to viral replication and cytokine release, and edema and protein deposition, which are induced by the strong inflammatory response and further impair alveolar function. Elevated angiotensin II levels may then lead to increased vascular permeability and promote microthrombus formation (8, 10, 11). Postmortem studies have shown that the lungs of affected patients resemble those of non-SARS-CoV-2 patients with acute respiratory distress syndrome (ARDS) (12), and a subset of COVID-19 patients display areas of atelectasis (13, 14).

Systemic treatment with dexamethasone can improve the outcome of severe COVID-19 (15), and the use of inhaled budesonide in early COVID-19 may reduce disease progression (16). Thus, understanding the mechanisms underlying the defective or dysregulated immune responses that occur in patients with severe COVID-19 is critical for combating the disease and for developing treatments for the most severely affected patients.

Recent studies have shown that SARS-CoV-2 infection induces autoantibodies against various cytokines and autoimmune disease-related proteins in patients with severe

AJRCCM Articles in Press. Published August 04, 2022 as 10.1164/rccm.202201-0011OC

disease (17-19). While these reports generally focus on immunoglobulin G (IgG), rapid and sustained production of immunoglobulin A (IgA) has been shown to occur during the early immune response to SARS-CoV-2 infection and in patients with severe COVID-19 (20, 21). These previously published observations provide a rationale for studying the role of IgA-driven autoreactivity in COVID-19 pathogenesis.

Kanduc et al. recently demonstrated similarities between the amino acid sequences of the SARS-CoV-2 spike protein and some human lung surfactant proteins (22), raising the possibility of autoreactivity to pulmonary surfactant proteins due to antigen mimicry (23, 24). Surfactant proteins are essential for maintaining respiratory physiology by promoting alveolar stability. Therefore, these results prompted us to ask whether patients with severe COVID-19 develop autoreactive IgA directed against pulmonary proteins, possibly affecting lung function and oxygenation status.

Some of the results of these studies have been previously reported in the form of a preprint (25).

Methods

Study Design and Sample Collection

We established a multicenter cross-sectional study at three Swiss and one German tertiary hospitals. For all patients, SARS-CoV-2 infection was detected by reverse-transcription polymerase chain reaction or rapid antigen testing and COVID-19 was clinically confirmed by the supervising physician (26). Severe COVID-19 was defined as respiratory insufficiency with oxygen supplementation due to SARS-CoV-2, while mild COVID-19 describes oligosymptomatic patients without the need for additional oxygen (27). We collected clinical data, blood, and lung tissue samples from patients with

AJRCCM Articles in Press. Published August 04, 2022 as 10.1164/rccm.202201-0011OC

severe COVID-19, patients with mild COVID-19 from April 2020 through April 2021. We further included pre-existing clinical data and biological material from non-infected healthy control patients, patients with bacterial pneumonia, and patients with influenza that had been collected between October 2017 and June 2020. Additionally, we obtained bronchoalveolar lavage fluid (BALF) samples from severe COVID-19 and non-COVID-19 patients, collected from March through November 2020. BALF collection and storage was performed as previously described (28).

Plasma and serum samples were isolated from whole blood collected into heparin-containing tubes (BD Vacutainer CPT tubes, Becton Dickinson) or serum tubes following centrifugation at 1,650xg for 20 minutes. The undiluted plasma or serum samples were then aliquoted and stored at -80°C. Postmortem lung tissue samples were collected and processed according to the local standard protocols.

We designated the first cohort with severe COVID-19 from the Cantonal Hospital St. Gallen as the derivation cohort (dCOVID), and a second, independent cohort from the University Hospital Basel as the validation cohort (vCOVID). Sample characterization, including type, quantities, and centers of collection is outlined in **Table S1**.

All patients gave informed consent for study participation and the study was performed in accordance with the Declaration of Helsinki guidelines. The study was approved by the responsible ethical committee at each study site (Swiss ethics protocol numbers 2020-01006, 2020-00566, 2020-00629, and 2020-00646, and Ethical Commission Tübingen number 259/2022BO2).

Identification of IgA-bound Proteins in BALF

AJRCCM Articles in Press. Published August 04, 2022 as 10.1164/rccm.202201-0011OC

To identify auto-IgA targeting pulmonary proteins, BALF samples were fixed and subsequently analyzed by liquid chromatography-tandem mass spectrometry. Preparation and analysis protocols are detailed in the **Methods** section of the online supplement.

Histology

To assess the presence of auto-IgA against SP-B and SP-C in lung tissue, double immunofluorescence stainings for IgA and SP-B/-C were performed. The staining strategy can be found in the **Methods** section of the online supplement.

ELISA Measurements

To identify auto-IgA against pulmonary surfactant proteins, we performed enzyme-linked immunosorbent assays (ELISAs) using recombinant proteins and poractant alfa (Curosurf, Chiesi Farmaceutici), a therapeutic porcine surfactant replacement. Our approach is described in the **Methods** section of the online supplement.

Surface Tension Measurement through Capillary Rise

To determine whether plasma or IgA from severe COVID-19 patients impairs surfactant function in vitro, we performed capillary rise measurements using poractant alfa. Details can be found in the **Methods** section of the online supplement.

Statistical Analyses

Data were analyzed using GraphPad Prism version 9.3.1. For two-group comparisons, the Mann-Whitney test was used, while for multiple-group comparisons the Kruskal-

AJRCCM Articles in Press. Published August 04, 2022 as 10.1164/rccm.202201-0011OC

Wallis test with Dunn's correction was applied. The Wilson/Brown method was used to perform area under the curve (AUC) receiver operating characteristics (ROC) analyses (29).

Results

Patient Characteristics

For blood sampling, we enrolled a total of 201 patients, of which 137 had severe COVID-19: 77 in the dCOVID cohort and 60 in the vCOVID cohort. 12 patients had mild COVID-19. 30 patients had bacterial pneumonia and were tested negative for SARS-CoV-2, and 22 individuals were healthy controls without SARS-CoV-2 infection. Clinical patient characteristics and demographics are listed in **Table 1**. The median age of dCOVID was 66 years, of vCOVID 70 years, and of bacterial pneumonia 69 years, whereas mild COVID-19 patients were younger (median 34 years). The average duration of hospitalization in the dCOVID and vCOVID cohorts was 15 days. Additionally, we received BALF from patients with severe COVID-19 (n=18), and from non-COVID-19 patients (n=18), and we collected formalin-fixed paraffin-embedded (FFPE) postmortem lung samples from 4 patients with severe COVID-19 and 5 patients, who did not have COVID-19.

Patients with Severe COVID-19 Harbor IgA Against SP-B and SP-C in their Lungs.

In line with previous reports, we found that ARDS in COVID-19 was frequently associated with alveolar collapse in histology (**Figure S1**). A major cause of alveolar collapse may be dysfunction of the pulmonary surfactant. We hypothesized that

AJRCCM Articles in Press. Published August 04, 2022 as 10.1164/rccm.202201-0011OC

autoantibodies disturb surfactant function and first investigated whether IgA targeting any pulmonary-associated proteins was detectable in BALF from severely ill patients. Using peptide-M agarose IgA purification followed by liquid chromatography-tandem mass spectrometry analysis, we identified proteins that were bound to IgA in BALF (**Figure 1A,B**). IgA was bound to surfactant protein B (SP-B) in 9 out of 18 (50%) patients, and SP-B was among the 30 most frequent proteins that were immunoprecipitated by our antigen detection approach. In comparison, SP-B was only detected in BALF from 3 out of 18 (17%) patients without COVID-19 and at lower overall levels (**Figure 1A**). The difference in IgA-bound BALF SP-B levels between COVID-19 and non-COVID-19 patients was statistically significant (*P=0.03, Mann-Whitney test) (**Figure 1C**). We next sought to determine whether these IgA were also present and co-localized with SP-B in the lungs of COVID-19 patients. To that end, we performed immunofluorescence staining on postmortem FFPE lung sections from dCOVID patients and compared them to lung tissue from non-COVID-19 patients with influenza or without viral infection (**Figure 2A**). All lung samples from the dCOVID cohort displayed the presence of IgA co-localized with SP-B within the alveoli (**Figure 2B**). In contrast, we did not detect any IgA in lung samples from patients with influenza (**Figure 2C**) or without viral infection (**Figure 2D**).

In its secreted form (sIgA), IgA exists as a dimer consisting of two monomers linked by a J-chain. A predominance of monomeric IgA in the lungs of severe COVID-19 patients could be the result of vascular damage, while sIgA would suggest a targeted immune reaction. Therefore, we performed an additional stain for the J-chain protein in these samples and found a strong signal only in the lungs of COVID-19 patients. This protein co-localized with SP-B and IgA, confirming the prominent presence of sIgA in these

AJRCCM Articles in Press. Published August 04, 2022 as 10.1164/rccm.202201-0011OC

samples (**Figure S2**). Since lung surfactant protein C (SP-C) is another key protein for lung surfactant function, we repeated the same staining with an SP-C-specific antibody and were able to detect IgA co-localizing with SP-C in lung tissue from COVID-19 patients (**Figure 3A**). As with SP-B, no IgA were detectable in lung tissue from influenza or uninfected patients (**Figure 3B,C**). Thus, COVID-19 pneumonitis was associated with the presence of autoreactive IgA against SP-B and SP-C in the lung.

IgA against SP-B and -C are Elevated in Blood Samples from Patients with Severe COVID-19. To determine whether autoantibodies against SP-B and other pulmonary surfactant proteins are also present in the blood of COVID-19 patients, we examined samples from dCOVID, mild COVID-19, and SARS-CoV-2-negative patients. First, we transduced human embryonic kidney (HEK293) cells with lentiviral vectors encoding the human surfactant proteins SP-A1, -A2, -B, -C, or -D, and confirmed their expressions by western blot (**Figure S3A**). Using pooled plasma from dCOVID (n=15) or mild COVID-19 (n=5) patients, we then performed indirect immunofluorescence staining for IgA on the transduced cells. We observed that patients with severe COVID-19 harbored much higher levels of anti-SP-B and -C IgA compared to those with mild COVID-19. Furthermore, IgA from both groups showed minimal to no binding to the other surfactant proteins, i.e., SP-A1, -A2, or -D (**Figure S3B**). These data demonstrate that the severity of COVID-19 correlates with the levels of anti-SP-B and SP-C IgA. We repeated this experiment with A549 lung adenocarcinoma cells, comparing plasma from the dCOVID (n=15) and non-infected control (n=5) cohorts. Here, we observed the same IgA staining pattern seen in HEK293 cells (**Figure S3C**). Analysis of the gene expression repository Lung Cell Atlas also revealed particularly high expression of SP-C (SFTPC) and SP-B

AJRCCM Articles in Press. Published August 04, 2022 as 10.1164/rccm.202201-0011OC

(SFTPB) in alveolar epithelial cells (30). Interestingly, SP-B and SP-C are both predominantly produced by type 2 pneumocytes, which are a key target cell type for SARS-CoV-2 (31).

Next, we assessed the levels of anti-surfactant IgA in patients with mild and severe COVID-19 via ELISAs using recombinant SP-B and SP-C (**Figure 4A**). We observed significantly higher levels of anti-SP-B and anti-SP-C IgA in plasma of patients with severe disease (dCOVID, n=77) compared to mild COVID-19 patients (n=12) and healthy controls (n=12) (**Figure 4B**). To confirm our observation with a clinically applied surfactant product, we coated our ELISA with poractant alfa (Curosurf, Chiesi Farmaceutici), a porcine lung surfactant used for intratracheal rescue therapy in preterm neonates with ARDS. As with the recombinant proteins, plasma from patients with severe COVID-19 presented significantly higher levels of surfactant-targeting IgA compared to plasma from non-infected patients. We then asked whether the levels of these IgA correlated with the clinical need for supplemental oxygen. Using ROC curves, we tested for thresholds that classified patients into severe versus mild COVID-19. Anti-SP-B- (AUC = 0.779), SP-C- (AUC = 0.751), and poractant alfa-IgA (AUC = 0.834) all showed area under the curve (AUC) values significantly above 0.5 (all ***$P < 0.001$). An absorption threshold at 0.054 for SP-B yielded a sensitivity of 79.2% and a specificity of 72.7%, a threshold at 0.056 for SP-C resulted in 79.2% sensitivity and 68.5% specificity, and a threshold for poractant alfa at 0.034 gave 70.8% sensitivity and 76.6% specificity (**Figure 4C**). Next, we sought to validate our auto-IgA findings in an independent vCOVID cohort and, additionally, investigated whether these IgA were COVID-19-specific by including a cohort of non-COVID-19 patients with severe bacterial

AJRCCM Articles in Press. Published August 04, 2022 as 10.1164/rccm.202201-0011OC

pneumonia. IgA against surfactant proteins were significantly elevated in the vCOVID cohort compared to bacterial pneumonia patients and uninfected controls. No significant difference was found between the IgA levels of patients with bacterial pneumonia and uninfected controls in any of the analyses (**Figure 4D**). These data strongly suggest that elevated IgA targeting surfactant proteins are specific for severe COVID-19.

To confirm that auto-IgAs were specifically targeting SP-B and SP-C, as shown with HEK293 and A549 cells (**Figure S3B,C**) rather than other surfactant proteins we repeated the ELISAs for IgA reactivity against SP-A and SP-D (**Figure S4**). While we did observe a significant difference between plasma samples from dCOVID and mild COVID-19 patients, there was no difference when comparing dCOVID to healthy control samples, indicating that the elevated signal seen in severe COVID-19 against SP-A and SP-D is not relevant (**Figure S4A,B**). When measuring IgA in vCOVID, bacterial pneumonia patients, and non-COVID-19 controls, no difference among the three groups was observed (**Figure S4C**).

Like other immunoglobulins, IgA can exhibit canonical (i.e., Fab-dependent) and non-canonical binding to antigens or target receptors (32). To examine whether the binding of IgA to surfactant proteins was canonical, we isolated IgA from a plasma pool of dCOVID patients (n=15) and performed antibody fragmentation with papain (33). ELISA with SP-B and SP-C using an Fc-specific horseradish peroxidase-conjugated secondary anti-human IgA antibody revealed significantly less signal compared to non-fragmented IgA. This supports the notion of a canonical binding of IgA to these proteins (**Figure S5A,B**). To explore whether the SP-B- and -C-binding IgA from blood are virus-specific and cross-target surfactant proteins due to molecular mimicry, we performed a competition assay. Virus-specific antibodies were blocked by pre-incubation of plasma

AJRCCM Articles in Press. Published August 04, 2022 as 10.1164/rccm.202201-0011OC

with SARS-CoV-2 lysate at a 20-fold excess compared to ELISA coating. Indeed, the absorbance signal was significantly reduced by an average of 22% for SP-B and 25% for SP-C after three replicates of ELISA (**Figure S5C**). While the signal reduction is modest, it is, nevertheless, likely caused by mimicry between viral and surfactant proteins.

Pulmonary Surfactant Function is Inhibited by Plasma and Isolated IgA from Patients with Severe COVID-19. We then assessed whether plasma and auto-IgA from patients with severe COVID-19 impaired the function of pulmonary surfactant, potentially contributing to alveolar collapse. First, we investigated if plasma from severe COVID-19 patients affected the surface tension of pulmonary surfactant using capillary rise measurements. Poractant alfa was incubated with pooled plasma from either dCOVID (n=15), mild COVID (n=5), or uninfected healthy control patients (n=5). Incubation with plasma from severe COVID-19 patients significantly increased surface tension compared to plasma from mild COVID-19 or uninfected control patients (**Figure 5A**). In contrast, there was no notable difference in surface tension when comparing incubation with plasma from mild COVID-19 patients or uninfected controls. To investigate whether IgA was the cause of this functional loss, we repeated the experiment with purified IgA from the dCOVID cohort (n=5). Concurringly, incubation with IgA resulted in significantly increased surface tension (**Figure 5B**). Taken together, these results strongly suggest that auto-IgA impair pulmonary surfactant function in severe COVID-19 patients (**Figure 5C**).

AJRCCM Articles in Press. Published August 04, 2022 as 10.1164/rccm.202201-0011OC

Discussion

COVID-19 continues to burden health care systems, and the mechanisms that contribute to disease progression remain poorly understood. Here, we demonstrate that anti-surfactant IgA in severe COVID-19 patients impair pulmonary surfactant proteins. While the presence of autoantibodies in COVID-19 has been reported (17, 19, 21), our data reveal a potential mechanistic driver of disease, as we show that auto-IgA interfere with the ability of pulmonary surfactant to lower surface tension. This could lead to impaired stabilization of the pulmonary air sacs, thus contributing to alveolar collapse and insufficient oxygen exchange (34). In an ongoing clinical trial with bovine surfactant (Alveofact®) for treatment of COVID-19 Postle *et al.* reported that pulmonary surfactant was compromised in patients with severe disease (35). Piva *et al*. showed that bronchoscopically administered poractant alfa as a surfactant replacement reduced the 28-day mortality of patients with severe COVID-19 (36). Avdeev *et al*. demonstrated that survivors of severe COVID-19 with surfactant substitution required less ventilation and were able to leave the hospital earlier than those without the replacement (37). These findings strongly suggest a crucial role of pulmonary surfactant in COVID-19. Antibodies targeting surfactant proteins have been associated with respiratory insufficiency in rabbits (38) and the addition of SP-B antibodies to surfactant in newborn rabbits lead to widespread alveolar collapse (39). Similarly, Kobayashi *et al*. reported that surfactant replacement therapy was ineffective for treating surfactant-deficient immature newborn rabbits when SP-B antibodies were added. In contrast, the addition of SP-A antibodies did not impair the function of supplementary surfactant (40, 41). Importantly, Losada-Olivia *et al*. recently investigated the effect of SARS-CoV-2 infection on pulmonary surfactant by comparing its activity in COVID-19 ARDS patients to non-COVID-19

AJRCCM Articles in Press. Published August 04, 2022 as 10.1164/rccm.202201-0011OC

ARDS patients. In line with our data, changes in pulmonary surfactant activity were only found in COVID-19 patients (42). Furthermore, ventilator-induced lung injury has been shown to impair pulmonary surfactant, possibly contributing to disease progression (43). J-chain co-localization with IgA in lungs of severe COVID-19 patients indicates that these are primarily sIgAs and, likely to a lesser extent, monomeric IgAs entering from damaged lung capillaries (44). These findings imply an expansion of local IgA-producing plasma cells, which is supported by a previous report showing a compartment-specific IgA production (45). Furthermore, it is possible that IgAs bind to other COVID-19-relevant proteins, such as antimicrobial peptides which are involved in defense against bacterial infection (46).

One limitation of our investigation is the number of enrolled patients. Additionally, access to longitudinal samples would allow us to analyze antibody level changes over time, including the effects of immunosuppressive therapies such as corticosteroids. Furthermore, surfactant protein reduction due to the destruction of type 2 pneumocytes by SARS-CoV-2 cannot be ruled out. However, as incubation of pulmonary surfactant with plasma from severe COVID-19 patients lead to an increase of surface tension, it is likely that auto-IgAs impact surfactant protein function. Given the region and time of our blood and tissue sample collection, we assume that most patients in our COVID-19 cohorts had been infected with either the SARS-CoV-2 wild type or Alpha (B.1.1.7) strain. It is possible that this pathomechanism depends on virus variants and should be further explored in future studies.

In summary, we identified SP-B- and SP-C-IgA in severe COVID-19 patients and demonstrated that auto-IgAs impair the capability of pulmonary surfactant to lower surface tension. Our data further strengthen the notion that IgA antibodies against self-

AJRCCM Articles in Press. Published August 04, 2022 as 10.1164/rccm.202201-0011OC

antigens in the lung corrupt crucial components of alveolar gas exchange, thereby providing novel mechanistic insights into the progression of COVID-19.

Acknowledgments

We are grateful to Dorothea Hillmann (Labormedizinisches Zentrum Dr. Risch) for her contributions to laboratory analyses. We also thank Drs. Lucy Robinson and Daniel Ackerman of Insight Editing London for critical review and editing of the manuscript. Graphical illustrations were prepared with BioRender (www.biorender.com).

Author disclosures

J.M.P. is founder and shareholder of Apeiron (Vienna, Austria), which develops soluble ACE2 as a COVID-19 therapy, and has no direct competing interest relating to this paper or data presented in the paper. All other authors have declared that no conflict of interest exists.

AJRCCM Articles in Press. Published August 04, 2022 as 10.1164/rccm.202201-0011OC

Figure Legends

Figure 1. SP-B IgA are found in BALF of severe COVID-19 patients. (**A**) Top 30 IgA-bound proteins in bronchoalveolar lavage fluid (BALF) of patients with severe COVID-19 (n=18) are presented in the left heatmap (red) and grouped by their respective physiological compartments. Each column represents a patient. The right heatmap (blue) shows results of IgA:protein precipitates of BALF from non-COVID-19 patients. Protein levels were normalized to the IgA heavy chain signals and $\log_2$ transformed. (**B**) Schematic workflow of the experimental setup for the identification of IgA-bound antigens. BALF was processed with peptide M pulldown columns, and IgA-bound proteins were measured and identified via liquid chromatography-tandem mass spectrometry. (**C**) Quantitative comparison revealed a significantly higher level of IgA:SP-B complexes in the severe COVID-19 versus non-COVID-19 BALF (*P = 0.03, Mann-Whitney test). Immunoprec., immunoprecipitate; norm., normalized.

Figure 2. Lungs of severe COVID-19 patients harbor co-localized SP-B and IgA. (**A**) Schematic of the staining strategy used to detect co-localization (merge = yellow) of IgA (FITC = green) with SP-B (Alexa 594 = red) in lung tissue from fatal COVID-19, influenza, or cancer patients by immunofluorescence. (**B**) Double immunofluorescence staining for SP-B and IgA in FFPE sections from lung tissue of patients with COVID-19 (n=4), (**C**) in biopsy specimens from patients with influenza (n=2), and (**D**) in uninfected patients with metastatic melanoma (n=3). Consistently, co-localization of SP-B with IgA was only observed in samples from deceased COVID-19 patients and not in the lungs of the other two groups. Scale bars = 100 µm.

AJRCCM Articles in Press. Published August 04, 2022 as 10.1164/rccm.202201-0011OC

Figure 3. Lungs of severe COVID-19 patients harbor co-localized SP-C and IgA. (**A**) Double immunofluorescence staining for SP-C (Alexa 594 = red) and IgA (FITC = green) in FFPE sections from lung tissue of patients with COVID-19 (n=4), (**B**) in biopsy specimens from patients with influenza (n=2), and (**C**) in uninfected patients with metastatic melanoma (n=3). Co-localization of SP-C with IgA was consistently seen only in samples from deceased COVID-19 patients and not in the lungs of the other two groups. Scale bars = 100 μm.

Figure 4. IgA targeting SP-B and -C are elevated in blood samples from patients with severe COVID-19. (**A**) Schematic representation of the IgA ELISA experiment using recombinant proteins as coating and diluted plasma from patients as the antibody source. TMB = substrate for horseradish peroxidase. (**B**) SP-B (left), SP-C (center), or poractant alfa (right) ELISAs revealed significantly more IgA against the target proteins in plasma from patients with severe COVID-19 (n=77) compared to those with mild COVID-19 (n=12) or healthy controls (n=12). (**C**) AUC-ROC analysis demonstrated that the presence of IgA against either SP-B (left), SP-C (center), or poractant alfa (right) was significantly associated with the requirement of the patient for oxygen supplementation. (**D**) Comparison of the surfactant-specific IgA levels in serum from vCOVID patients (n=60), patients with bacterial pneumonia and without SARS-CoV-2 infection (n=30), and non-infected control patients without pneumonia (n=10). ELISAs consistently detected significantly higher levels of IgA against SP-B (left), SP-C (center), and poractant alfa (right) in patients with severe COVID-19 compared to patients without COVID-19. All data are represented as mean ± 95% CI. For multiple

AJRCCM Articles in Press. Published August 04, 2022 as 10.1164/rccm.202201-0011OC

comparisons, the Kruskal-Wallis test with Dunn's correction was used (NS, not significant; *P < 0.05; **P < 0.01; ***P < 0.001; ****P < 0.0001).

Figure 5. Plasma and isolated IgA from severe COVID-19 patients inhibit the function of pulmonary surfactant. (**A**) Incubation of poractant alfa (40 mg/mL) with plasma from severe COVID-19 patients resulted in a significant increase of surface tension, whereas plasma from mild COVID-19 and non-infected healthy control patients did not experience notable changes. (**B**) Purified IgA (0.2 mg/mL) from plasma of severe COVID-19 patients (n=5) caused a significant increase of surface tension compared to PBS controls (n=3). (**C**) Graphical summary of our results showing that auto-IgA occur in the alveoli and blood of severely diseased COVID-19 patients, bind to surfactant proteins, and cause impairment of pulmonary surfactant function. All data are represented as mean ± SD. For single comparisons, a Mann-Whitney test was used, and for multiple comparisons, a Kruskal-Wallis test with Dunn's correction was applied (NS, not significant; *P < 0.05; **P < 0.01).

AJRCCM Articles in Press. Published August 04, 2022 as 10.1164/rccm.202201-0011OC

Table 1. Clinical characteristics of patients.

Characteristic	Severe COVID-19 Derivation cohort (dCOVID) (n=77)	Severe COVID-19 Validation cohort (vCOVID) (n=60)	Mild COVID-19 (n=12)	Bacterial Pneumonia (n=30)
Sex, male - no./total (%)	55/77 (71)	46/60 (77)	4/12 (33)	18/30 (60)
Median age (IQR) - yrs	66 (60-73)	70 (62-79)	34 (32-48)	69 (59-78)
Median days of hospitalization (IQR)	15 (10-25)	15 (11-23)	n/a	n/a
Oxygen supplementation - no./total (%)	77/77 (100)	60/60 (100)	0/12 (0)	17/30 (57)
Intubation	20/77 (26)	53/60 (88)	0 (0)	n/a
ECMO	10/77 (13)	2/60 (3)	0 (0)	n/a
Other (nasal, mask)	47/77 (61)	5/60 (8)	0 (0)	n/a
Comorbidities[*]- no./total (%)	71/77 (92)	54/60 (90)	3/12 (25)	23/30 (77)
Hypertension	50/77 (65)	37/60 (62)	2/12 (17)	15/30 (50)
Cardiovascular disease	14/77 (18)	24/60 (40)	0/12 (0)	15/30 (50)
Diabetes	29/77 (38)	30/60 (50)	1/12 (8)	2/30 (7)
Obesity[†]	52/77 (68)	28/60 (47)	1/12 (8)	8/30 (27)
Autoimmune disease	9/77 (12)	6/60 (10)	1/12 (8)	n/a
Cancer	8/77 (10)	6/60 (10)	2/12 (17)	n/a
Haematological disorder	6/77 (8)	12/60 (20)	2/12 (17)	n/a
Immunosuppression[‡] - no./total (%)	76/77 (99)	n/a	1/12 (8)	n/a
Laboratory parameters[§]				
Median CRP level - mg/l (IQR)	194 (107-254)	125 (68-173)	n/a	n/a
No. of patients with data	77	60	n/a	n/a
Median D-dimer level - mg/l (IQR)	2.2 (1.1-9.9)	1.3 (0.9-2.6)	n/a	n/a
No. of patients with data	68	53	n/a	n/a
Median leukocyte count - G/l (IQR)	13.9 (10.5-19.6)	9.1 (5.4-13.5)	n/a	n/a
No. of patients with data	76	60	n/a	n/a

AJRCCM Articles in Press. Published August 04, 2022 as 10.1164/rccm.202201-0011OC

*Only co-morbidities considered relevant for COVID-19 outcome are included and listed.

†Obesity is defined as a Body Mass Index of ≥25.

‡Immunosuppression is defined as any of the following: systemic prednisone ≥7.5mg/day (or equivalent), interleukin inhibitors (such as tocilizumab), other systemic immunosuppressive drugs (e.g., calcineurin inhibitors), or chemotherapy. All therapies had been established prior to treatment of COVID-19.

§Laboratory parameters are included where available. Number of patients with available values are provided in the consecutive row. For each patient and parameter, the highest value measured during hospitalization was used.

ECMO, extracorporeal membrane oxygenation; CRP, C-reactive protein; IQR, interquartile range; n/a, data not available; SARS-CoV-2, severe acute respiratory syndrome coronavirus 2; yrs, years.

AJRCCM Articles in Press. Published August 04, 2022 as 10.1164/rccm.202201-0011OC

References

1. Lane HC, Fauci AS. Research in the Context of a Pandemic. N Engl J Med 2021;384:755-757.

2. Wiersinga WJ, Rhodes A, Cheng AC, Peacock SJ, Prescott HC. Pathophysiology, Transmission, Diagnosis, and Treatment of Coronavirus Disease 2019 (COVID-19): A Review. JAMA 2020;324:782-793.

3. Dagan N, Barda N, Kepten E, Miron O, Perchik S, Katz MA*, et al.* BNT162b2 mRNA Covid-19 Vaccine in a Nationwide Mass Vaccination Setting. N Engl J Med 2021;384:1412-1423.

4. Baden LR, El Sahly HM, Essink B, Kotloff K, Frey S, Novak R*, et al.* Efficacy and Safety of the mRNA-1273 SARS-CoV-2 Vaccine. N Engl J Med 2021;384:403-416.

5. Voysey M, Clemens SAC, Madhi SA, Weckx LY, Folegatti PM, Aley PK*, et al.* Safety and efficacy of the ChAdOx1 nCoV-19 vaccine (AZD1222) against SARS-CoV-2: an interim analysis of four randomised controlled trials in Brazil, South Africa, and the UK. Lancet 2021;397:99-111.

6. Lopez Bernal J, Andrews N, Gower C, Gallagher E, Simmons R, Thelwall S*, et al.* Effectiveness of Covid-19 Vaccines against the B.1.617.2 (Delta) Variant. N Engl J Med 2021;385:585-594.

7. Patel MD, Rosenstrom E, Ivy JS, Mayorga ME, Keskinocak P, Boyce RM*, et al.* Association of Simulated COVID-19 Vaccination and Nonpharmaceutical Interventions With Infections, Hospitalizations, and Mortality. JAMA Netw Open 2021;4:e2110782.

AJRCCM Articles in Press. Published August 04, 2022 as 10.1164/rccm.202201-0011OC

8. Tay MZ, Poh CM, Renia L, MacAry PA, Ng LFP. The trinity of COVID-19: immunity, inflammation and intervention. Nat Rev Immunol 2020;20:363-374.

9. Leisman DE, Mehta A, Thompson BT, Charland NC, Gonye ALK, Gushterova I*, et al.* Alveolar, Endothelial, and Organ Injury Marker Dynamics in Severe COVID-19. Am J Respir Crit Care Med 2022;205:507-519.

10. Fajgenbaum DC, June CH. Cytokine Storm. N Engl J Med 2020;383:2255-2273.

11. Ni W, Yang X, Yang D, Bao J, Li R, Xiao Y*, et al.* Role of angiotensin-converting enzyme 2 (ACE2) in COVID-19. Crit Care 2020;24:422.

12. Grasselli G, Tonetti T, Protti A, Langer T, Girardis M, Bellani G*, et al.* Pathophysiology of COVID-19-associated acute respiratory distress syndrome: a multicentre prospective observational study. Lancet Respir Med 2020;8:1201-1208.

13. Mingote A, Albajar A, Garcia Benedito P, Garcia-Suarez J, Pelosi P, Ball L*, et al.* Prevalence and clinical consequences of atelectasis in SARS-CoV-2 pneumonia: a computed tomography retrospective cohort study. BMC Pulm Med 2021;21:267.

14. Bosmuller H, Matter M, Fend F, Tzankov A. The pulmonary pathology of COVID-19. Virchows Arch 2021;478:137-150.

15. Horby P, Lim WS, Emberson JR, Mafham M, Bell JL, Linsell L*, et al.* Dexamethasone in Hospitalized Patients with Covid-19. N Engl J Med 2021;384:693-704.

16. Ramakrishnan S, Nicolau DV, Jr., Langford B, Mahdi M, Jeffers H, Mwasuku C*, et al.* Inhaled budesonide in the treatment of early COVID-19 (STOIC): a phase 2, open-label, randomised controlled trial. Lancet Respir Med 2021;9:763-772.

AJRCCM Articles in Press. Published August 04, 2022 as 10.1164/rccm.202201-0011OC

17. Wang EY, Mao T, Klein J, Dai Y, Huck JD, Jaycox JR*, et al.* Diverse functional autoantibodies in patients with COVID-19. Nature 2021;595:283-288.

18. Chang SE, Feng A, Meng W, Apostolidis SA, Mack E, Artandi M*, et al.* New-onset IgG autoantibodies in hospitalized patients with COVID-19. Nat Commun 2021;12:5417.

19. Bastard P, Rosen LB, Zhang Q, Michailidis E, Hoffmann HH, Zhang Y*, et al.* Autoantibodies against type I IFNs in patients with life-threatening COVID-19. Science 2020;370:eabd4585.

20. Sterlin D, Mathian A, Miyara M, Mohr A, Anna F, Claer L*, et al.* IgA dominates the early neutralizing antibody response to SARS-CoV-2. Sci Transl Med 2021;13:e2223.

21. Hasan Ali O, Bomze D, Risch L, Brugger SD, Paprotny M, Weber M*, et al.* Severe COVID-19 is associated with elevated serum IgA and antiphospholipid IgA-antibodies. Clin Infect Dis 2020:ciaa1496.

22. Kanduc D, Shoenfeld Y. On the molecular determinants of the SARS-CoV-2 attack. Clin Immunol 2020;215:108426.

23. Martinez-Calle M, Parra-Ortiz E, Cruz A, Olmeda B, Perez-Gil J. Towards the Molecular Mechanism of Pulmonary Surfactant Protein SP-B: At the Crossroad of Membrane Permeability and Interfacial Lipid Transfer. J Mol Biol 2021;433:166749.

24. Serrano AG, Perez-Gil J. Protein-lipid interactions and surface activity in the pulmonary surfactant system. Chem Phys Lipids 2006;141:105-118.

25. Sinnberg T, Lichtensteiger C, Hasan Ali O, Pop OT, Gilardi M, Risch L*, et al.* IgA autoantibodies target pulmonary surfactant in patients with severe COVID-19

AJRCCM Articles in Press. Published August 04, 2022 as 10.1164/rccm.202201-0011OC

[preprint]. 2021 [accessed 2022 Jul 18]. Available from: https://www.medrxiv.org/content/medrxiv/early/2021/02/07/2021.02.02.21250940.full.pdf.

26. Lieberman JA, Pepper G, Naccache SN, Huang ML, Jerome KR, Greninger AL. Comparison of Commercially Available and Laboratory-Developed Assays for In Vitro Detection of SARS-CoV-2 in Clinical Laboratories. J Clin Microbiol 2020;58.
27. Gandhi RT, Lynch JB, Del Rio C. Mild or Moderate Covid-19. N Engl J Med 2020;383:1757-1766.
28. Buehler PK, Zinkernagel AS, Hofmaenner DA, Wendel Garcia PD, Acevedo CT, Gomez-Mejia A*, et al.* Bacterial pulmonary superinfections are associated with longer duration of ventilation in critically ill COVID-19 patients. Cell Rep Med 2021;2:100229.
29. Brown LD, Cai TT, DasGupta A. Interval Estimation for a Binomial Proportion. Statist Sci 2001;16:101-133.
30. Vieira Braga FA, Kar G, Berg M, Carpaij OA, Polanski K, Simon LM*, et al.* A cellular census of human lungs identifies novel cell states in health and in asthma. Nat Med 2019;25:1153-1163.
31. Monteil V, Kwon H, Prado P, Hagelkruys A, Wimmer RA, Stahl M*, et al.* Inhibition of SARS-CoV-2 Infections in Engineered Human Tissues Using Clinical-Grade Soluble Human ACE2. Cell 2020;181:905-913.e907.
32. Pabst O, Slack E. IgA and the intestinal microbiota: the importance of being specific. Mucosal Immunol 2020;13:12-21.
33. Andrew SM, Titus JA. Fragmentation of immunoglobulin G. Curr Protoc Cell Biol 2003;Chapter 16:Unit 16.4.

AJRCCM Articles in Press. Published August 04, 2022 as 10.1164/rccm.202201-0011OC

34. Ochs M, Timm S, Elezkurtaj S, Horst D, Meinhardt J, Heppner FL*, et al.* Collapse induration of alveoli is an ultrastructural finding in a COVID-19 patient. Eur Respir J 2021;57:2004165.

35. Postle AD, Clark HW, Fink J, Madsen J, Koster G, Panchal M*, et al.* Rapid Phospholipid Turnover after Surfactant Nebulization in Severe COVID-19 Infection: A Randomized Clinical Trial. Am J Respir Crit Care Med 2022;205:471-473.

36. Piva S, DiBlasi RM, Slee AE, Jobe AH, Roccaro AM, Filippini M*, et al.* Surfactant therapy for COVID-19 related ARDS: a retrospective case-control pilot study. Respir Res 2021;22:20.

37. Avdeev SN, Trushenko NV, Chikina SY, Tsareva NA, Merzhoeva ZM, Yaroshetskiy AI*, et al.* Beneficial effects of inhaled surfactant in patients with COVID-19-associated acute respiratory distress syndrome. Respir Med 2021;185:106489.

38. Strayer DS, Herting E, Sun B, Robertson B. Antibody to surfactant protein A increases sensitivity of pulmonary surfactant to inactivation by fibrinogen in vivo. Am J Respir Crit Care Med 1996;153:1116-1122.

39. Robertson B, Kobayashi T, Ganzuka M, Grossmann G, Li WZ, Suzuki Y. Experimental neonatal respiratory failure induced by a monoclonal antibody to the hydrophobic surfactant-associated protein SP-B. Pediatr Res 1991;30:239-243.

40. Kobayashi T, Nitta K, Takahashi R, Kurashima K, Robertson B, Suzuki Y. Activity of pulmonary surfactant after blocking the associated proteins SP-A and SP-B. J Appl Physiol (1985) 1991;71:530-536.

AJRCCM Articles in Press. Published August 04, 2022 as 10.1164/rccm.202201-0011OC

41. Kobayashi T, Robertson B, Grossmann G, Nitta K, Curstedt T, Suzuki Y. Exogenous porcine surfactant (Curosurf) is inactivated by monoclonal antibody to the surfactant-associated hydrophobic protein SP-B. Acta Paediatr 1992;81:665-671.

42. Sanchez-Ortiz D, Mingote A, Castejon R, Hernandez G, Diaz G, Echaide M*, et al.* Pulmonary Surfactant Activity and Surfactant Protein SP-B Levels in COVID-19-Related Acute Respiratory Distress Syndrome [abstract]. Am J Respir Crit Care Med 2022;205:A3212.

43. Albert RK. Constant Vt Ventilation and Surfactant Dysfunction: An Overlooked Cause of Ventilator-induced Lung Injury. Am J Respir Crit Care Med 2022;205:152-160.

44. Johansen FE, Braathen R, Brandtzaeg P. The J chain is essential for polymeric Ig receptor-mediated epithelial transport of IgA. J Immunol 2001;167:5185-5192.

45. Sterlin D, Mathian A, Miyara M, Mohr A, Anna F, Claer L*, et al.* IgA dominates the early neutralizing antibody response to SARS-CoV-2. Sci Transl Med 2021;13:eabd2223.

46. Schnapp D, Harris A. Antibacterial peptides in bronchoalveolar lavage fluid. Am J Respir Cell Mol Biol 1998;19:352-356.

AJRCCM Articles in Press. Published August 04, 2022 as 10.1164/rccm.202201-0011OC

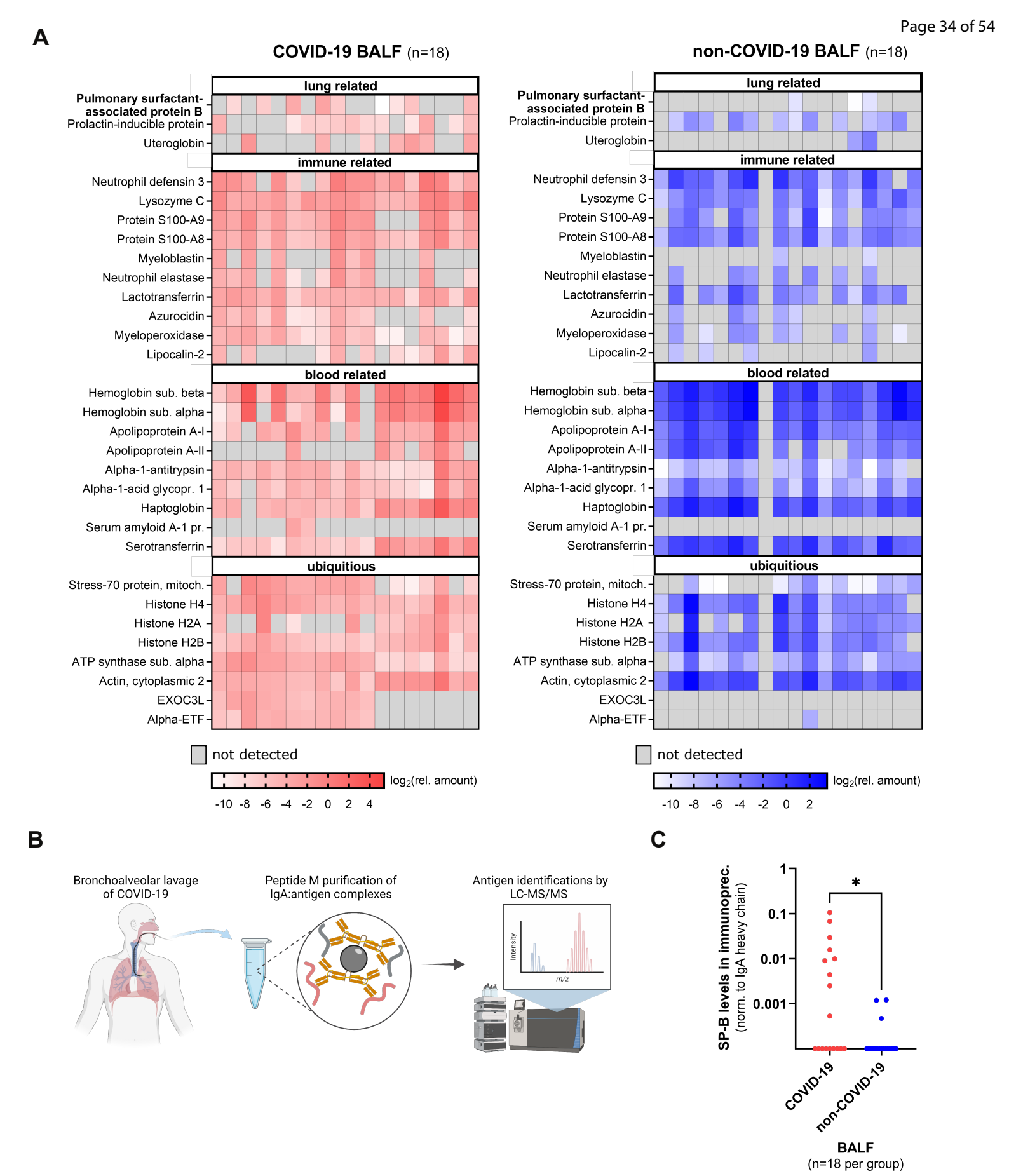

AJRCCM Articles in Press. Published August 04, 2022 as 10.1164/rccm.202201-0011OC

Figure 1

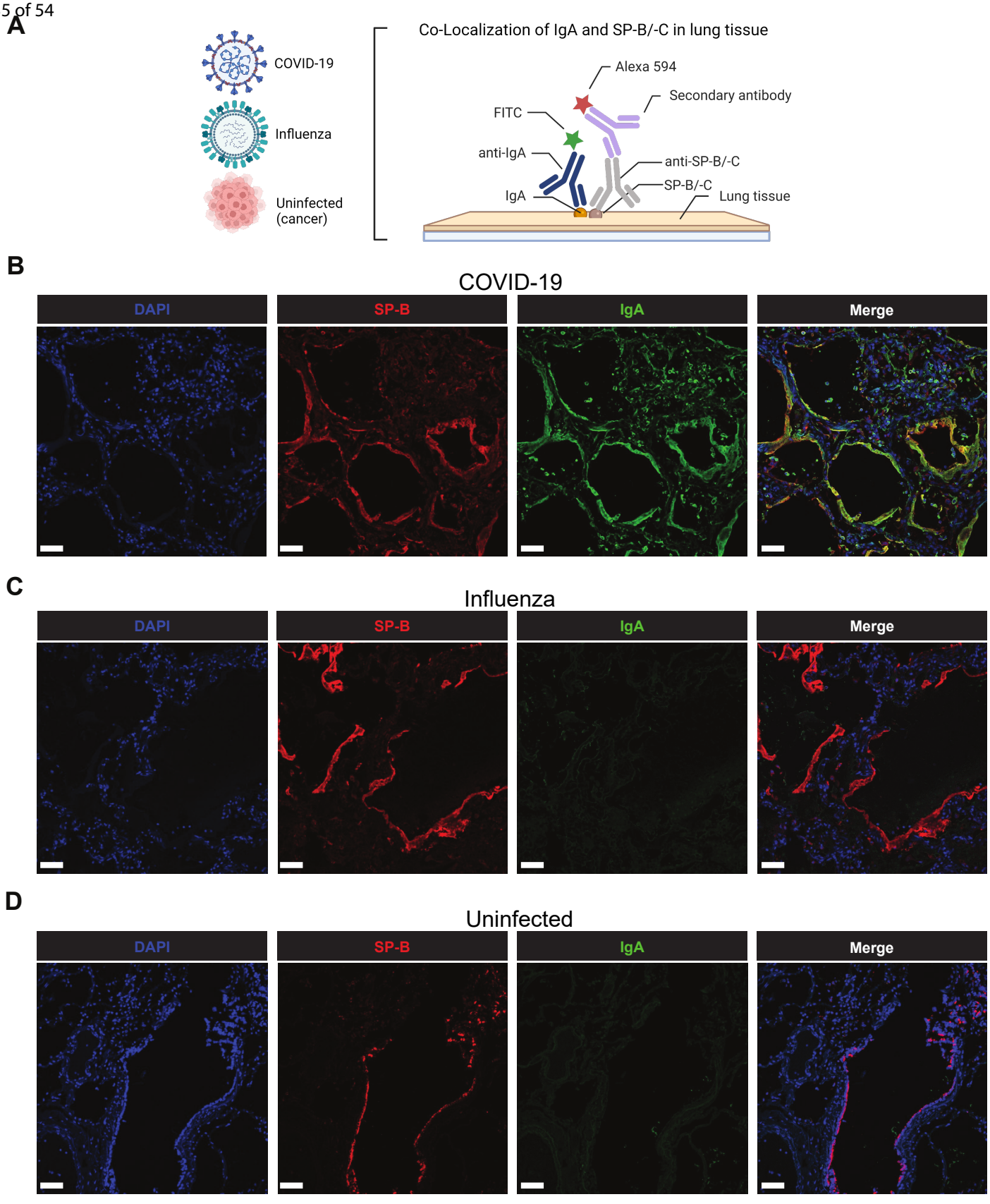

AJRCCM Articles in Press. Published August 04, 2022 as 10.1164/rccm.202201-0011OC

Figure 2

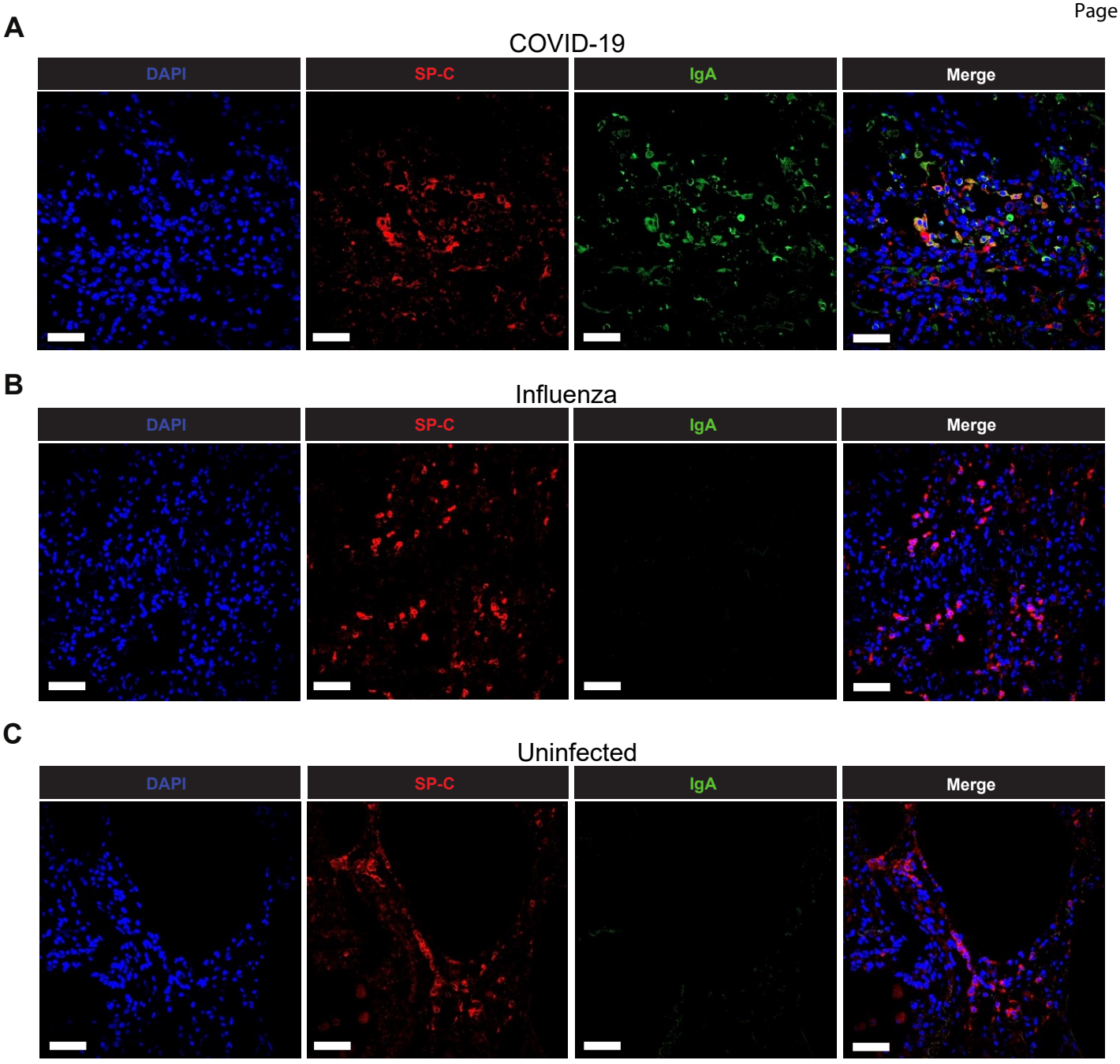

AJRCCM Articles in Press. Published August 04, 2022 as 10.1164/rccm.202201-0011OC

Figure 3

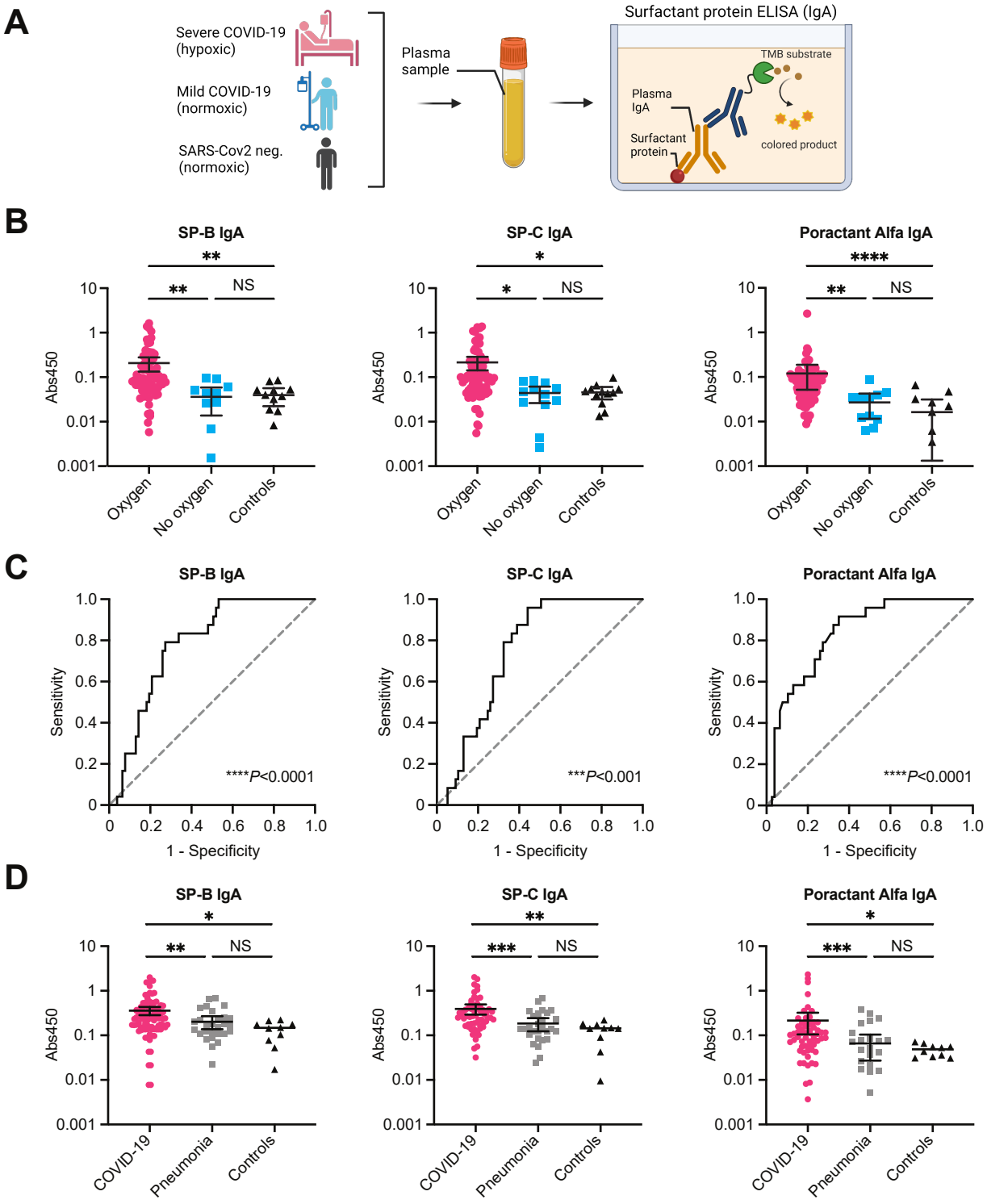

AJRCCM Articles in Press. Published August 04, 2022 as 10.1164/rccm.202201-0011OC

Figure 4

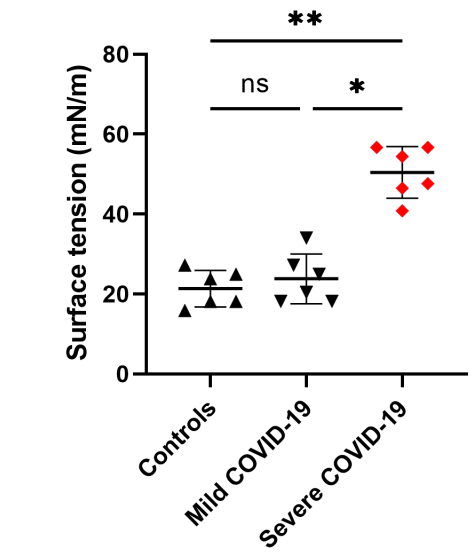

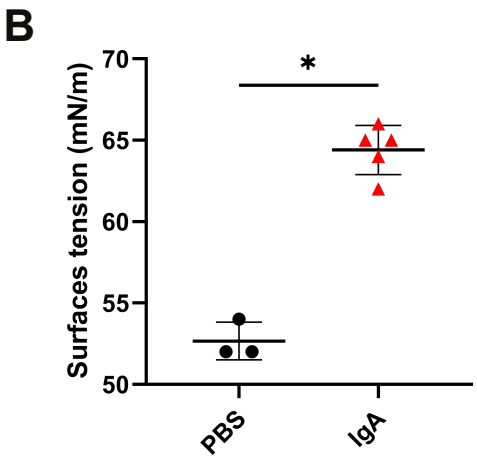

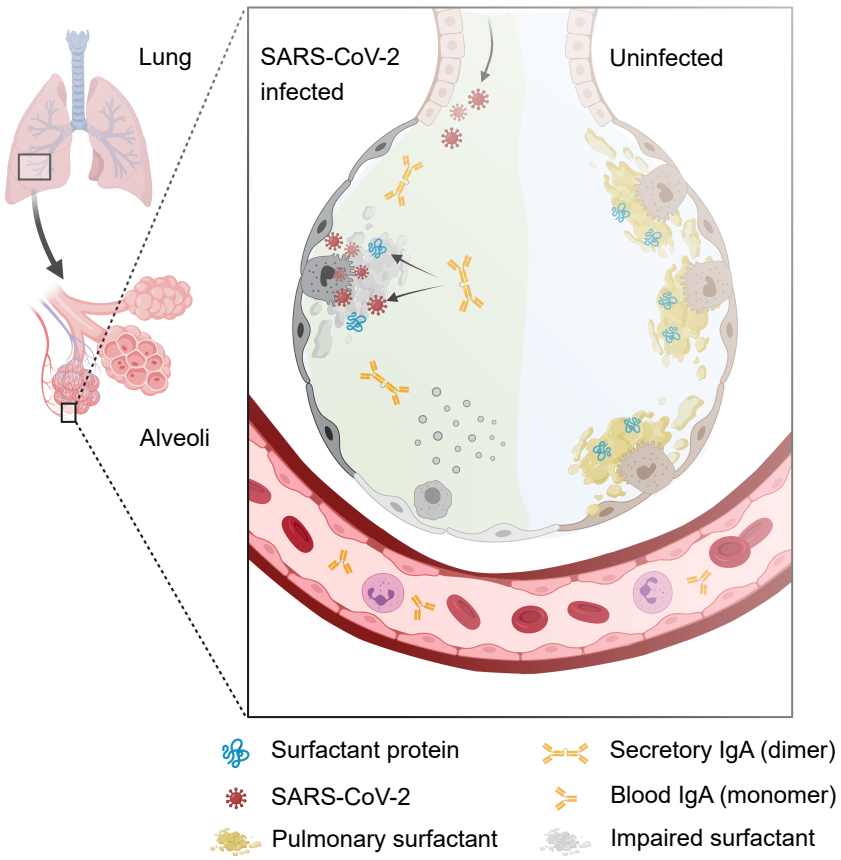

AJRCCM Articles in Press. Published August 04, 2022 as 10.1164/rccm.202201-0011OC

Figure 5

Supplemental information

Pulmonary surfactant proteins are inhibited by IgA autoantibodies in severe COVID-19

Tobias Sinnberg, Christa Lichtensteiger, Omar Hasan Ali, Oltin T. Pop, Ann-Kristin Jochum, Lorenz Risch, Silvio D. Brugger, Ana Velic, David Bomze, Philipp Kohler, Pietro Vernazza, Werner C. Albrich, Christian R. Kahlert, Marie-Therese Abdou, Nina Wyss, Kathrin Hofmeister, Heike Niessner, Carl Zinner, Mara Gilardi, Alexandar Tzankov, Martin Röcken, Alex Dulovic, Srikanth Mairpady Shambat, Natalia Ruetalo, Philipp K. Bühler, Thomas C. Scheier, Wolfram Jochum, Lukas Kern, Samuel Henz, Tino Schneider, Gabriela M. Kuster, Maurin Lampart, Martin Siegemund, Roland Bingisser, Michael Schindler, Nicole Schneiderhan-Marra, Hubert Kalbacher, Kathy D. McCoy, Werner Spengler, Martin H. Brutsche, Boris Maček, Raphael Twerenbold, Josef M. Penninger, Matthias S. Matter, and Lukas Flatz

Supplementary Methods

Identification of IgA-bound proteins in BALF by LC-MS/MS:
BALF samples were fixed and incubated on ice for 90 minutes with 20% paraformaldehyde/2% glutaraldehyde solution in HEPES buffer pH 7.0, at a 1:10 v/v ratio, to inactivate SARS-CoV-2 and form protein cross-links. To halt the fixation process, 200 µL of 1 M Tris pH 8.0 per mL of solution was added. For immunoprecipitation of Ig and bound proteins within BALF, 750 µL of each sample was diluted in 10 mL of PBS buffer and brought to a volume of 500 µL through a 30 kD spin column (Vivaspin, Sartorius). 75 µL of a PBS-pre-equilibrated 50% peptide M slurry (Invivogen) per BALF sample was incubated in mini-spin columns on a roller mixer for 2 hours before centrifugation at 1,000x g for one minute to remove unbound proteins. After five wash steps with 500 µL PBS each, samples were eluted by adding 200 µL 2x Laemmli buffer and centrifuging as above. 150 µL of the eluted samples were separated by short-term SDS-PAGE prior to mass spectrometric analysis. In-gel digestion with

AJRCCM Articles in Press. Published August 04, 2022 as 10.1164/rccm.202201-0011OC

trypsin was conducted as previously described (1). Extracted peptides were desalted using C18 StageTips and subjected to liquid chromatography with tandem mass spectrometry (LC-MS/MS) analysis. LC-MS/MS analyses were performed on an Easy-nLC 1200 UHPLC (Thermo Fisher Scientific) coupled to an Orbitrap Exploris 480 mass spectrometer (Thermo Fisher Scientific) as previously described (2). Peptides were eluted with a 60-minute segmented gradient at a flow rate of 200 nL/min, selecting the 20 most intensive peaks for fragmentation with higher-energy C-trap dissociation. The MS data were processed with MaxQuant software suite v.1.6.7.047 to measure the intensity based absolute quantification (iBAQ), which was used to calculate the relative protein level normalized to the iBAQ of the C regions of the alpha chain of IgA (IGHA1 and IGHA2). Database search was provided against human (96817 entries) UniProt database using the Andromeda search engine.

Histology with SP-B & IgA immunofluorescence:

Lung tissue samples were fixed in formalin and embedded in paraffin using standard processing protocols. Four-micron-thick serial sections were cut using a RM2255 rotary microtome (Leica Biosystems) and placed on poly-L-lysine-coated slides. The slides were dewaxed in xylene, rehydrated and stained using hematoxylin & eosin (H&E, both Dako) or subjected to heat-induced epitope retrieval in a microwave oven using a pH 6 target retrieval solution for 20 minutes, allowed to cool to room temperature (RT), then incubated for 60 minutes with 1x PBS/0.1% Tween-20/5% skimmed milk at RT. Excess liquid was removed and a mouse anti-human surfactant precursor protein B antibody (Leica Biosystems, Cat. No. NCL-SPPB, 1:100) was added overnight at 4 °C. Slides were then incubated for 1 hour at RT with a donkey anti-mouse-A594 antibody (Jackson, Cat. No. 715-585-150, 1:200) in 1x PBS 0.1% Tween-20, followed by another 1-hour incubation at RT with rabbit anti-human IgA FITC (Dako, Cat. No. F0204, 1:50). After washing, slides were counterstained with DAPI and mounted using fluorescence mounting medium (Dako, Cat. No. S3023). All fluorescence images were acquired using a LSM 980 confocal microscope with Airyscan 2 (Zeiss). Whole slide scans of H&E-stained FFPE lung tissue sections were acquired with a Panoramic 250 Flash III digital

AJRCCM Articles in Press. Published August 04, 2022 as 10.1164/rccm.202201-0011OC

slide scanner (3D Histech) and processed using the CaseViewer 2.4 software (3D Histech).

Surfactant protein C & IgA immunofluorescence:
Slides were dewaxed in xylene, rehydrated, and subjected to heat-induced epitope retrieval in a sodium citrate solution (pH 6) for 20 minutes in a microwave oven. Slides were then allowed to cool to RT, followed by a 60-minute incubation with 1x PBS/1% Triton-X/5% skimmed milk at RT. Excess liquid was removed and sections were incubated for 18 hours at 4 °C with a rabbit anti-human (pro-) surfactant protein C antibody (Abcam, Cat. No. ab90716, 1:200) in 1x PBS/1% Triton-X followed by a 1-hour incubation at room RT with an Alexa Fluor 594 goat anti-rabbit IgG (H+L) antibody (Jackson Immunoresearch, Cat. No. 111-585-003, 1:200) in 1x PBS/1% Triton-X. Slides were then incubated for 1 hour at RT with a polyclonal rabbit anti-human IgA/FITC antibody (Agilent, Cat. No. F020402-2, 1:50) in 1x PBS/1% Triton-X, counterstained with DAPI, and mounted using fluorescence mounting medium (Dako, Cat. No. S3023).

Surfactant protein B & IgA & J chain immunofluorescence:
Slides were dewaxed in xylene, rehydrated, and subjected to heat-induced epitope retrieval in a sodium citrate solution (pH 6) for 20 minutes in a microwave oven. Slides were then allowed to cool to room temperature followed by an avidin/biotin blocking step (15 minutes each) using an Avidin/Biotin Bloking Kit (Vector Laboratories, Cat. No. SP-2001) and a 60-minute incubation with 1x PBS/1% Triton-X/5% skimmed milk at RT and. Excess liquid was removed and sections were incubated for 18 hours at 4 °C with a polyclonal rabbit anti-human J chain antibody (Invitrogen, Cat. No. PA5-83707, 1:500) in 1x PBS/1% Triton-X, followed by a 1-hour incubation at RT Alexa Fluor 594 goat anti-rabbit IgG (H+L) antibody (Jackson Immunoresearch, catalog number 111-585-003, dilution1:400) in 1x PBS/1% Triton-X. This was followed by another incubation for 18 hours at 4 °C with a monoclonal mouse anti-human (pro-) surfactant protein B antibody (Novocastra, Cat. No. NCL-L-SPPB, 1:200), a 1-hour incubation at RT with a biotinylated anti-Mouse secondary antibody (GBI labs, Cat. No. D31-1, 1:400) in 1x PBS/1% Triton-X, and a 1-hour incubation at RT with Alexa Fluor 647 streptavidin

AJRCCM Articles in Press. Published August 04, 2022 as 10.1164/rccm.202201-0011OC

(Jackson Immunoresearch, Cat. No. 016-600-984, 1:400) in 1x PBS/1% Triton-X. Slides were then incubated for 1 hour at RT with a polyclonal rabbit anti-human IgA/FITC antibody (Agilent, Cat. No. F020402-2, 1:50) in 1x PBS/1% Triton-X, counterstained with DAPI, and mounted using fluorescence mounting medium (Dako, Cat. No. S3023).

ELISA Measurements:

5 µL poractant alfa (Curosurf, Chiesi) or 200 ng of pulmonary surfactant-associated protein B or C (OriGene Technologies, Cat. No. TP324088 or Cat. No. TP303246, respectively; or in-house expressed in HEK293 cells and affinity-purified) were coated in 100 µL of 0.05 M carbonate-bicarbonate buffer, pH 9.6 per well using 96-well flat-bottom MediSorp plates (Thermo Fisher Scientific) at 4 °C overnight. Plates were washed once with 225 µL ELISA wash buffer (PBS + 0.05% Tween-20), and 150 µL ELISA blocking buffer (PBS + 10% normal human goat sera) was added to the wells. Plates were incubated for 3 hours at RT. ELISA blocking buffer was removed from the wells and 1:200 dilutions of sample plasma in 100 µL ELISA blocking buffer with 0.05% Tween-20 were added to each well in duplicates. Plates were incubated for 1 hour at RT. Plates were washed 4 times with 225 µL ELISA wash buffer and 1:2,000 goat anti-human IgA HRP (Jackson Immune Research, Cat. No. 109-035-011) in 100 µL ELISA blocking buffer with 0.05% Tween-20 added to the wells. Plates were incubated for 1 hour at RT. Plates were washed 4 times with 225 µL ELISA wash buffer. 70 µL TMB substrate (Cell Signaling Technology) was added to the wells and plates were incubated for 20-30 minutes in the dark at RT. 70 µL 1 M sulfuric acid was added to the wells and absorbance at 450 nm was measured in a TriStar microplate reader (Berthold Technologies). Competition with viral proteins was performed by preincubation of the diluted plasma samples with 10 µg/µL of SARS-CoV-2 wild type (lineage B.1) lysate or 10 µg/mL BSA in lysis buffer as control for 30 minutes at RT before adding the plasma to the antigen-coated ELISA plate. Viral lysate and BSA in lysis buffer (0.5% Triton X-100) were used at stock concentrations of 0.5 mg/mL.

Surface Tension Measurement through Capillary Rise:

AJRCCM Articles in Press. Published August 04, 2022 as 10.1164/rccm.202201-0011OC

40 mg/mL of PBS-diluted poractant alfa was mixed in a 1:1 ratio with pooled plasma from healthy controls (n=5), mild COVID patients (n=5), or dCOVID patients (n=15), and incubated at 37 °C for 30 minutes. For IgA assays, 10 mg/mL poractant alfa was mixed with 0.2 mg/mL immunopurified IgA from dCOVID patients and incubated as above. Pure 1x PBS was used as reference. The surface tension was determined as previously described (3). Briefly, a 5 µL glass capillary (Blaubrand micropipettes, Brand) was placed vertically into a tube filled with 50 µL of each solution. The height of the liquid column and the radii of the ellipsoidal meniscus at the air-liquid interface in the capillary were measured after 5 minutes with a digital microscope (DigiMicroscope USB 200, Reflecta GmbH). The surface tension was then calculated using the following formula (p_l: solution density; g: acceleration caused by gravity; h_{min}: solution column height at the lower level of the meniscus):

$$\gamma = \rho_l g h_{min} \frac{{R_x}^2}{2R_z}$$

Surfactant-associated Protein overexpressing HEK293 and A549 Cells:
HEK293 cells (purchased from CLS Cell Lines Service, Cat. No. 300192) or A549 cells (ATCC, Cat. No. CRM-CCL185) were transduced with lentiviral particles encoding the surfactant-associated proteins A1 (NM_005411), A2 (NM_205854), B (NM_000542), C (NM_003018) and D (NM_003019) (RC220332L3V, RC217867L3V, RC207605L3V, RC203246L3V, RC204746L3V, Origene) and selected with 0.5 µg/mL puromycin (Invivogen) for three passages. The cells were further expanded, and HEK293 cells were used for affinity purification of over-expressed proteins via the encoded Flag tag (Anti-FLAG M2 Affinity gel, Merck) using a chromatography system (Äkta pure 25 L1, Cytiva) or lysed and immunoblotted for the detection of Flag-tagged surfactant-associated proteins using the monoclonal anti-Flag BioM2 antibody (Merck) at a dilution of 1:2,000. HRP-linked anti-mouse IgG antibody at 1:3,000 served as the secondary antibody (Cell Signaling Technology) and was detected by chemiluminescence (Pierce ECL Western Blotting Substrate, Thermo Fisher Scientific) using an Imager 600 (GE Amersham). For assaying the binding of IgA antibodies in pooled serum from patients with severe COVID-19 from the dCOVID cohort (n=15), or mild COVID-19 (n=5), or non-COVID-19 patients (n=5), 40,000 transduced HEK293 or A549 cells were seeded in

AJRCCM Articles in Press. Published August 04, 2022 as 10.1164/rccm.202201-0011OC

each cavity of 4-chambered cell culture slides (Corning). The next day, medium was removed and cells were briefly (5 minutes) fixed with 4% buffered formaldehyde. Cells were blocked for 15 minutes with PBS,1% BSA before incubation with plasma pools (1:50 in blocking solution) for 30 minutes at RT. After three washes with PBS, the IgA bound to the cells was detected using ready-to-use Fluorescein-labeled anti-human IgA conjugate (Inova Diagnostics) before mounting with 1,4-diazabicyclo[2.2.2]octane-containing mounting medium and fluorescence detection using an Axiovert 200 fluorescence microscope (Zeiss).

Papain Cleavage of Antibodies:

Plasma pools from patients with COVID-19 were used to isolate immunoglobulins using 1 mL Capto L resin (Cytiva) packed into Chromabond empty columns (Macherey-Nagel) as recommended by the manufacturer. 5 mg of isolated immunoglobulins from patients with severe COVID-19 or mild COVID-19 were dialyzed against sample buffer (20 mM sodium phosphate, 10 mM EDTA, pH 7.0) and incubated in digestion buffer (sample buffer with 20 mM L-cysteine) with agarose-immobilized papain (Thermo Fisher Scientific) at 37 °C overnight with interval mixing. 10 µL of the digest were analyzed on a 10% SDS-PAGE gel and stained with Coomassie Brilliant Blue R-250 Staining Solution as recommended by the manufacturer (Bio-Rad). ELISAs against SP-B and SP-C were performed to test the effect of papain cleavage on the detection of antigen-bound IgA using an alpha-chain-specific HRP-conjugated anti-IgA.

Supplementary References:

1. Borchert N, Dieterich C, Krug K, Schutz W, Jung S, Nordheim A, et al. Proteogenomics of Pristionchus pacificus reveals distinct proteome structure of nematode models. *Genome Res* 2010; 20: 837-846.
2. Theurillat I, Hendriks IA, Cossec JC, Andrieux A, Nielsen ML, Dejean A. Extensive SUMO Modification of Repressive Chromatin Factors Distinguishes Pluripotent from Somatic Cells. *Cell Rep* 2020; 32: 108146.
3. Huck-Iriart C, De-Candia A, Rodriguez J, Rinaldi C. Determination of Surface Tension of Surfactant Solutions through Capillary Rise Measurements: An Image-

AJRCCM Articles in Press. Published August 04, 2022 as 10.1164/rccm.202201-0011OC

Processing Undergraduate Laboratory Experiment. *Journal of Chemical Education* 2016; 93: 1647-1651.

AJRCCM Articles in Press. Published August 04, 2022 as 10.1164/rccm.202201-0011OC

Table S1. Sample characteristics

Cohort	Type	Number	Origin
Severe COVID-19 Derivation cohort (dCOVID)	Plasma	77	Cantonal Hospital St. Gallen
Postmortem severe COVID-19	Lung tissue	5	
Mild COVID-19 Derivation cohort	Plasma	12	
Healthy controls	Plasma	12	
Postmortem non-COVID-19 controls	Lung tissue	4	
Severe COVID-19 Validation cohort (vCOVID)	Serum	60	University Hospital Basel
Bacterial pneumonia	Serum	30	
Healthy controls	Serum	10	
Severe COVID-19	BALF*	18	University Hospital Zurich
Non-COVID-19 controls	BALF	18	University Hospital Tübingen

*BALF, bronchoalveolar lavage fluid

AJRCCM Articles in Press. Published August 04, 2022 as 10.1164/rccm.202201-0011OC

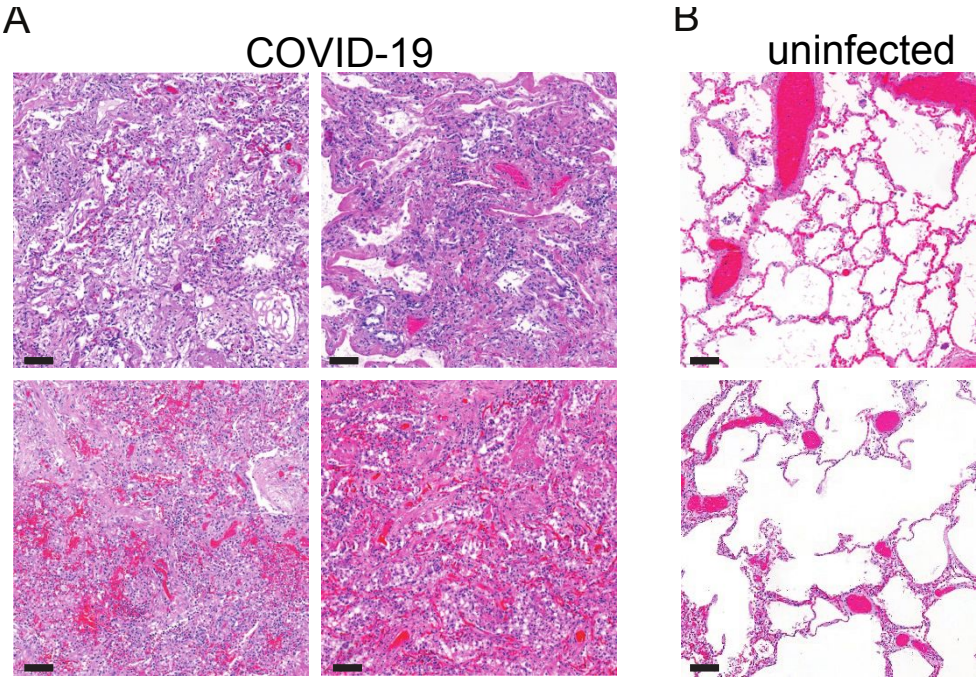

Figure S1. Lung histology of COVID-19. Post-mortem lung tissue samples from COVID-19 patients were compared to non-cancerous areas of lungs from non-COVID-19 patients with lung adenocarcinoma. (**A**) Representative micrographs of H&E-stained FFPE lung tissue sections from patients infected with SARS-CoV-2. In addition to diffuse alveolar damage, edema, and fibrosis, alveolar collapse was also observed in four out of five COVID-19 patients. (**B**) Histology of non-infected lungs showing open alveoli and normal epithelial lining with type I and II pneumocytes on a thin basal lamina. Scale bars = 100 μm.

AJRCCM Articles in Press. Published August 04, 2022 as 10.1164/rccm.202201-0011OC

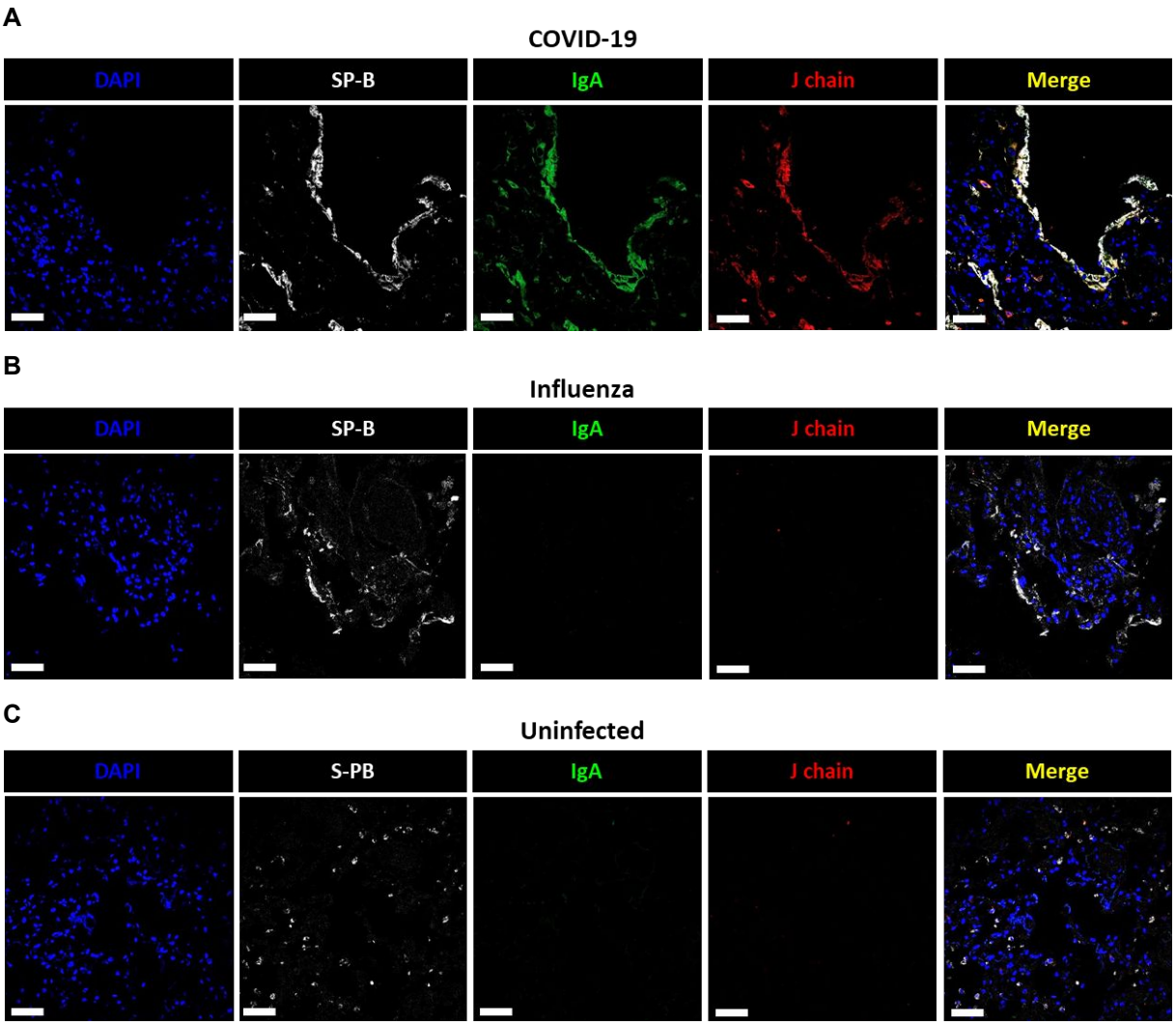

Figure S2. COVID-19 lung tissue contains secreted/dimeric IgA. (**A**) Immunofluorescence staining shows that secreted IgA with J chains co-localize with SP-B only in patients with severe COVID-19 (n=4). Lung tissues from patients with (**B**) influenza (n=2) or (**C**) pre-pandemic lungs from melanoma patients (n=3) do not show presence of IgA. Scale bars = 100 μm.

AJRCCM Articles in Press. Published August 04, 2022 as 10.1164/rccm.202201-0011OC

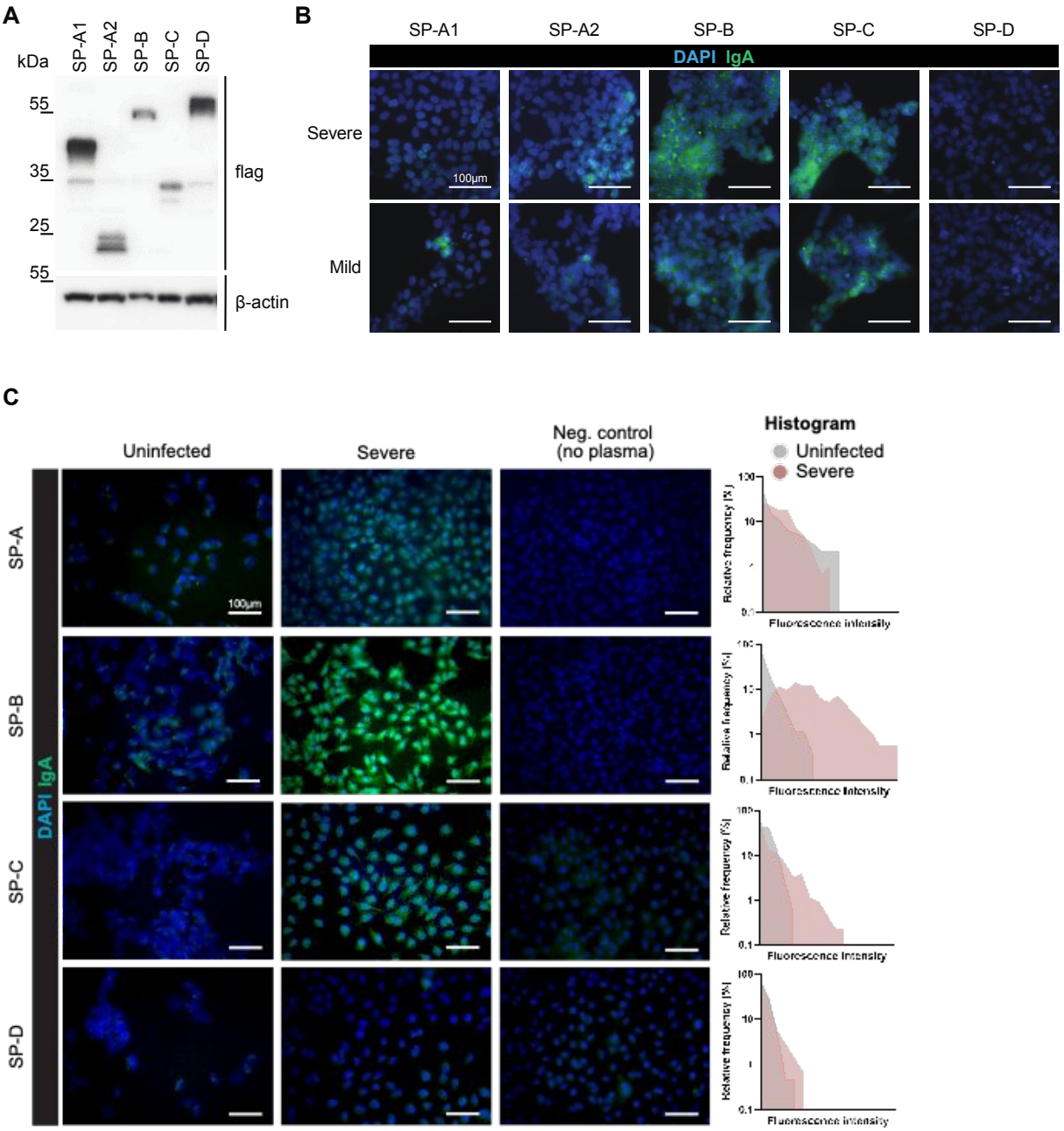

Figure S3. IgA autoantibodies specifically bind to SP-B and SP-C in patients with severe COVID-19. (**A**) HEK293 cells were transduced with lentiviral particles encoding SP-A1, -A2, -B, -C or -D (left to right). Western blotting confirmed the expression of each protein using FLAG-tags. Beta-actin served as the loading control (bottom). (**B**) The transduced HEK293 cells were incubated with pooled plasma from patients from the dCOVID (n=15, top panel) or mild COVID-19 (n=8, bottom panel) cohorts.

AJRCCM Articles in Press. Published August 04, 2022 as 10.1164/rccm.202201-0011OC

Immunofluorescence labeling showed a pronounced IgA signal for SP-B and SP-C, but not for the other surfactant proteins. (**C**) A549 cells were transduced in the same manner as the HEK293 cells. These cells were then incubated with pooled plasma from patients in the dCOVID (n=15, middle column) and non-infected control (n=5, left column) cohorts. Anti-IgA-FITC fluorescence intensity was quantified using CellProfiler software (v4.2.1). Mean fluorescence intensities were analyzed per cell and plotted as a histogram.

AJRCCM Articles in Press. Published August 04, 2022 as 10.1164/rccm.202201-0011OC

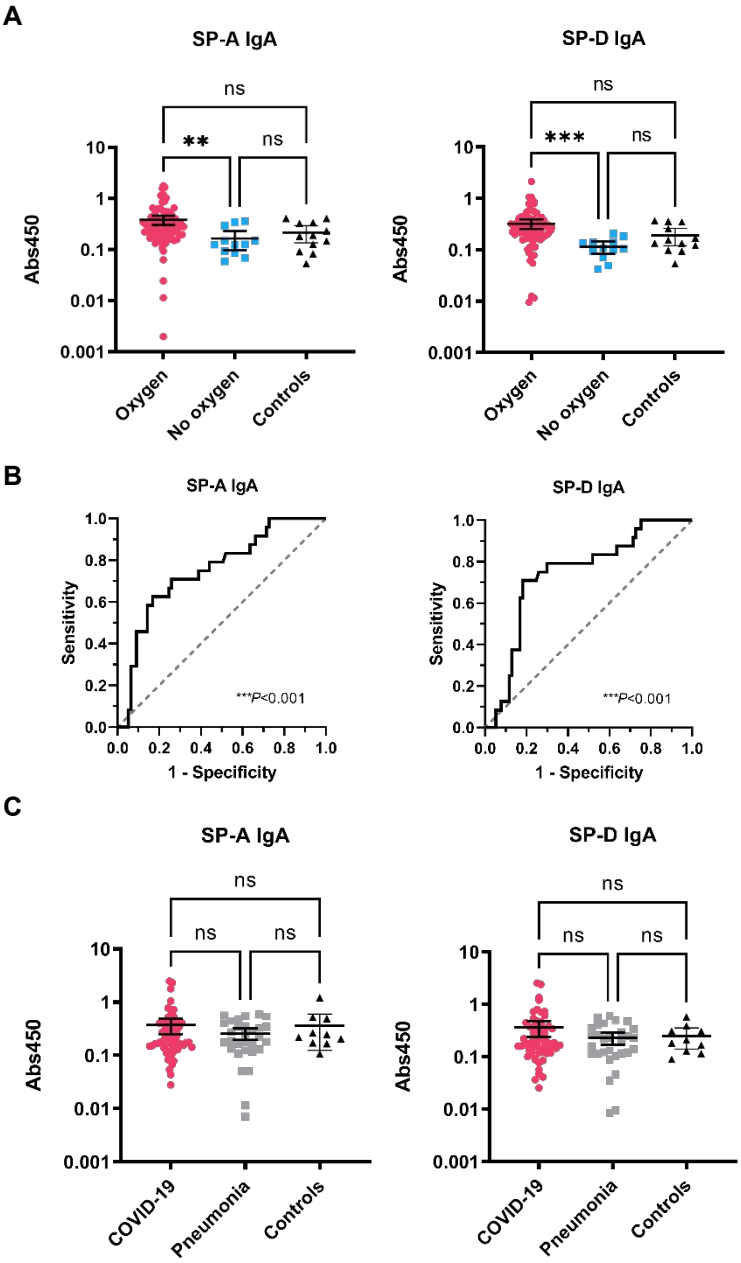

Figure S4. IgA targeting SP-A and -D are not consistently elevated in blood samples from patients with severe COVID-19. (**A**) IgA ELISA with recombinant SP-A (left) and SP-D (right) as coating, using diluted plasma from dCOVID patients with oygen need (n=77); mild COVID-19 patients without additional oxgen (n=12); healthy controls (n=12) as the antibody sources. (**B**) AUC-ROC analysis using the absorption values of SP-A or SP-D IgA ELISA and the need of the corresponding patient for oxygen supplementation (**C**) SP-A and -D specific IgA ELISA using serum from vCOVID

AJRCCM Articles in Press. Published August 04, 2022 as 10.1164/rccm.202201-0011OC

patients (n=60); bacterial pneumonia patients (n=30); and non-infected controls (n=10) as the antibody sources. All data are represented as mean with 95% CI. For multiple comparisons, two-way ANOVA with Tukey's multiple comparisons test used (ns, not significant; $^{**}P < 0.01$; $^{***}P < 0.001$).

AJRCCM Articles in Press. Published August 04, 2022 as 10.1164/rccm.202201-0011OC

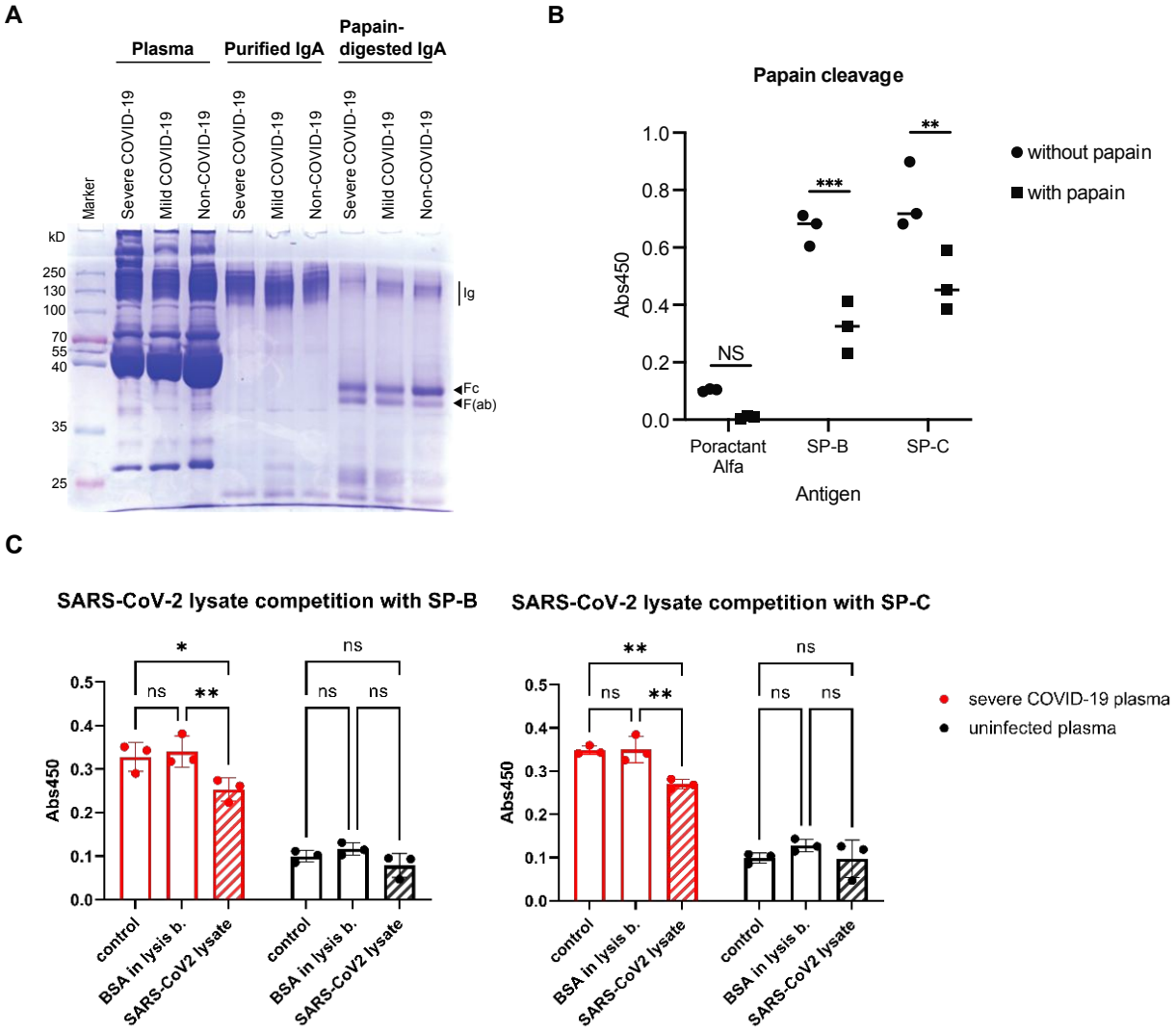

Figure S5. Blood IgA from severe COVID-19 patients exhibit canonical binding to SP-B and SP-C with their antigen-binding fragments. (**A**) Coomassie stained SDS-PAGE gel showing proteins from plasma (left), peptide M-purified IgA (center), and papain-digested IgA (right). After papain digestion, the Fc- and Fab-fragments are separately visible. Plasma from dCOVID patients (n=15) and patients with mild COVID-19 (n=5) was pooled randomly. (**B**) ELISA with SP-B and SP-C shows a significant reduction of IgA signal after papain digestion. The secondary antibody (anti-human IgA) binds to the Fc-region of IgA, indicating that only the Fab-region of IgA remains attached to the antigen. Data in triplicates are shown with the median, comparing poractant alfa, SP-B, and SP-C with and without papain using the two-way ANOVA with

AJRCCM Articles in Press. Published August 04, 2022 as 10.1164/rccm.202201-0011OC

Šídák multiple comparisons test; ns, not significant; **P < 0.01; ***P < 0.001. **(C)** Competition ELISA with SARS-CoV-2 lysate (10 µg/mL) compared to BSA in lysis buffer (10 µg/mL), which were used to compete with plasma antibodies in the pooled severe COVID-19 plasma samples (n=15). Data are shown as mean absorption values ±SD of three replicate ELISA assays, **P < 0.01; ***P < 0.001, two-way ANOVA with Tukey multiple comparisons test.

AJRCCM Articles in Press. Published August 04, 2022 as 10.1164/rccm.202201-0011OC